SUPRAMOLECULAR CHIRAL SELF-ASSEMBLED PEPTIDE NANOSTRUCTURES

A DISSERTATION SUBMITTED TO
THE GRADUATE SCHOOL OF ENGINEERING AND SCIENCE
OF BILKENT UNIVERSITY
IN PARTIAL FULFILLMENT OF THE REQUIREMENTS FOR
THE DEGREE OF
MASTER OF SCIENCE
IN
MATERIALS SCIENCE AND NANOTECHNOLOGY

By

Meryem Hatip

January 2016

SUPRAMOLECULAR CHIRAL SELF-ASSEMBLED PEPTIDE NANOSTRUCTURES

By Meryem Hatip

January, 2016

We certify that we have read this thesis and that in our opinion it is fully adequate, in scope and in quality, as a dissertation for the degree of Master of Science.

_____

Mustafa Özgür Güler (Advisor)

_____

Ayşe Begüm Tekinay

_____

Emine Deniz Tekin

Approved for the Graduate School of Engineering and Science

_____

Levent Onural

Director of the Graduate School

ABSTRACT

SUPRAMOLECULAR CHIRAL SELF-ASSEMBLED PEPTIDE NANOSTRUCTURES

Meryem Hatip

M.Sc. in Materials Science and Nanotechnology

Advisor: Assoc. Prof. Dr. Mustafa Özgür Güler

January, 2016

Self-assembly process is an easy and convenient bottom-up technique for designing novel functional materials. Self-assembled peptide amphiphile (PA) molecules are remarkable building blocks for a wide-range of applications due to their easy synthesis, biocompatibility, biodegradabability and dynamic nature in aqueous conditions.

Controlling self-assembly behavior still remains complex, since it can be affected by multiple factors. Chirality is an important parameter for designing and controlling self-assembled supramolecular nanomaterials. In this thesis, self-assembly mechanism of chiral peptide molecules was studied with different driving forces in order to develop new methodsfor producing self-assembled nanomaterials. In addition to self-assembly mechanism, different morphologies and chiral behaviors of the self-assembled supramolecular chiral peptide amphiphile nanostructureswere monitored with variouscharacterization methods.

pH is a significant contributor for the self-assembly process and this effect was studied in detail to elucidate pH dependency of supramolecular conformation. According to morphological characterizati^{o}ns, histidine containing PA molecules form nanosheet like structures under acidic pH.At the isoelectric point of imidazole, they have a tendency to form twisted fiber or ribbon structures. Athigh pH

conditions, pH 10, they form nanotubes due to the neutralization of imidazole groups and π-π interactionsat theside chain of histidine moiety.When another aromatic ring is included in the sequence, in this case phenylalanine residue, different nanostructures were observed.

In addition to histidine PA, lysine and glutamic acid containing peptide building blocks were also studied to understand the effect of electrostatic interactions. Phenylalanine containing PAs and valine containing PAs were compared in terms of their chiral self-assembly behaviors. As a result of self-assembly of the positively charged and negatively charged peptides, well defined nanostructures were obtained. While valine containing PA molecules form straight nanofibers, phenyl alanine containing PAs form well ordered rigid twisted fibers and twisted ribbon structures.

Keywords: peptide, self-assembly, nanostructured materials, programmed self-assembly, tuning morphology, nanofiber, nanotube, circular dichroism, twisted β-sheet, nanotechnology.

ÖZET

KENDİLİĞİNDEN DÜZENLENEN SUPRAMOLEKÜLER KİRAL PEPTİT NANOYAPILAR

Meryem Hatip

Malzeme Bilimi ve Nanoteknoloji Programı, Yüksek Lisans

Tez Danışmanı: Doç. Dr. Mustafa Özgür Güler

Ocak, 2016

Kendiliğinden bir araya gelme işlemi, yeni biyomedikal malzemeler üretmek için kullanılan kolay ve işlevsel bir tekniktir. Kendiliğinden bir araya gelen peptit amfifiller; kolay sentezlenebilmeleri, biyouyumlu, biyobozunur özellikleri ve sudaki dinamik yapıları sayesinde bu alanda sıklıkla kullanılan yapı taşlarıdır.

Bu tezde, peptit amfifil kiral supramolaküler nanoyapıların, farklı tetikleyici güçlerle kendiliğinden bir araya gelme mekanizmaları çalışılmıştır. Kendiliğinden bir araya gelme mekanizmalarının yanında, oluşturdukları farklı morfolojiler, kiral davranışlar, farklı karakterizasyon teknikleriyle takip edilmiştir.

Bu tezin ilk kısmında,pH değerinin kendiliğinden bir araya gelme mekanizmasına etkisi histidin içeren kiral peptit amfifillerle çalışmıştır. Yapısal karakterizasyonlara göre, asidik değerlerde histidin içeren peptit amfifil nanoyapılar oluşturmalarına rağmen, imidazol grubunun isoelektrik noktasına yakın değerlerde, bu yapılar nanofiber ve nanokurdele yapılara dönüşmektedir. pH 10 gibi yüksek pH değerlerinde, bu moleküller imidazol gruplarının nötrlenmesi ve π-π etkileşiminin baskın hale gelmesi sonucunda nanotüp gibi yapılar oluşturmaktadırlar. Buna karşılık, peptit sekansına başka bir aromatik halkanın eklenmesiyle bu organizasyon gözlemlenmemiştir.

Histidin içeren PA moleküllere ek olarak, lisin ve glutamik asit içeren yapı taşlarının yük nötrlenmesiyle kendiliğinden bir araya gelmesi de çalışılmıştır. Bu çalışmalarla,

aromatik halka içeren PA moleküler ile aromatik olmayan moleküllerin, kiral davranışları, morfolojileri, kendiliğinden bir araya gelme mekanizmaları kıyaslanmıştır. Aromatik olmayan PA molekülleri düz nanofiber yapılar oluştururken, fenil alanin grubu içeren aromatik PA molekülleri iyi düzenlenmiş, dönerli nanofiber ve kurdele benzeri nanoyapılar oluşturmaktadırlar.

Anahtar Kelimeler: peptit, kendiliğinden bir araya gelme, nanoyapılı morfoloji kontrol, nanofiber, nanotüp, dairesel dikroism, kıvrımlı β-yaprak, nanoteknoloj

Acknowledgement

I would like to thank to everyone who contributed to my MS thesis. First, I would like to thank to my advisor Prof. Mustafa Özgür Güler for his guidance. I am sincerely grateful to Prof. Ayşe B. Tekinay for an active collaboration and fruitful discussions. I would like to thank to my colleagues and my senior peersDr. Ruslan Garifullin, Mohammad Aref Khalily, Göksu Çinar, Elif Arslan, Gülcihan Gülseren for helpful discussions. I am thankful to The Scientific and Technological Research Council of Turkey (TÜBİTAK) for BİDEB 2215 fellowship and TÜBİTAK grant number 114Z728.

I would like to expressmost sincere thanks to friends;mydearest friendAygül Zengin, my old friend Gülcihan Gülseren, my perfect travelmates;Gülistan Tansık, Elif Arslan, Berna Şentürk and Mevhibe Geçer. Their support always motivated me. In addition, special thanks to my officemates, Hepi Hari Susapto, Melis Şardan Zeynep Aytaç, Aslı Çelebioğlu, Yelda Ertaş, Fatma Kayacı, Zehra İrem Gürbüz. They helped me to work in such a warm environment.

I would like to thank to Dr.Özlem Erol, Hatice Kübra Kara, Özüm Sehnaz Günel,Alper Devrim Özkan, Ahmet Emin Topal, Egemen Deniz Eren Seren Hamsici, Oya İlke Şentürk, Fatma Begüm Dikeçoğlu and other former and current members of the Biomimetic Materials Laboratory (BML) and Nanobiotechnology group for sharing knowledge and providing excellent support. This thesis could not be written without the support I have had from them.

I would like to thank toMustafa Güler and Zeynep Erdoğan for technical assistance and helpful discussion.

I would like to special thank to my best buddies, Zeynep Tuna, Mehtap Safi and Elif Solmaz. We sharedunforgettable memories together and I always felt their support including my undergraduate years. Another special thanks toCansu Kaya, Darika Okeev, Tuğçe Karataş, Merve Demirkıran, and Esra Soner for their companionship in this chemistry marathon.

I am immeasurably grateful to my family. Firstly I would like to thank my father Dr. Ömer Etka Hatip, he is my first role model in academic life. He always understands

my struggles and constantly encouraged me during my study. Then my mother Ayşe Hatip, she has always been the first to support and love me. I would like to thank my brothers Ahmet Halit and Mustafa Emre, my sisters Betül and Şeyma.

I would like to thank three little girls Elif, Nur and Mavi. They always fill my hearth with joy.

Finally, I would like to foremost thank to God, whose many blessing have made me who I am today.

Contents

List of Figures

List of Schemes

List of Tables

Chapter 1

Introduction

1.1. Peptide Synthesis

1.1.1 Peptide Chemistry

Peptides are small building blocks that consist of short amino acid chains. Peptide synthesis was based on well-known peptide bond formation between two amino acids. This covalent bond formed as a result of dehydration reaction between carboxyl group (C-terminus) of one amino acid which reacts the amino group (N-terminus) of another amino acid. (Figure-1.1).

Although peptides can be isolated from plants, animals or bacteria, synthesis of peptides in laboratory environment provides infinite diversity in design of both natural and unnatural amino acids. The first step of peptide synthesis was first performedby Theodor Curtius in1881. He used the azide-coupling method, and produced the first N-protected dipeptide, benzoylglycylglycine. But his work was not published. The first published work in this area belongs to Emil Fischer. However, he synthesized the first synthetic dipeptide, glycylglycin, in solution phase. Although that was the beginning of peptide chemistry[1, 2]development of solid phase peptide synthesis (SPPS) by Robert Bruce Merrifield[3]was the most important milestone. The new strategy, which was the amino acid construction on small beads in a stepwise manner, has eliminated many drawbacks of the solution phase synthesis such as low yield during synthesis, difficulty of deprotection of functional sides, removal of by-

products and so on. Merrifield's revolutionary contribution to chemistry field was awarded with Nobel Prize in 1984. [3,4]Today, his method is the most widely used alternative for traditional solution phase peptide synthesis.

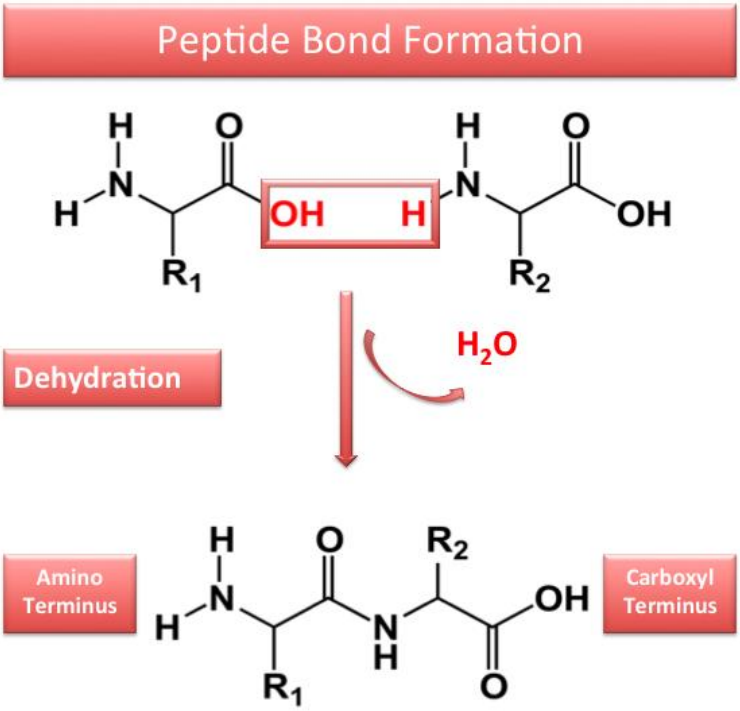

Figure 1.1 Peptide bond formation

A major element in solid phase peptide synthesis (SPPS) isthe polymeric solid resin, on which the amino acid sequences assemble.[5,6]These resins are treated with a large number of functional units, and every single amino acid covalently attaches atthese units. The principle of the SPPS method is based on the stepwise addition of the N-protected C-terminus amino acids to the systems. Each step consists of deprotection-washing-coupling-washingcycles. The protecting group of the first amino acid, which isalready loaded to the resin, gets broken, and carboxyl side of the second amino acid reacts with only this unprotected free amine side. While peptide grows in solid resin, excess of coupling reagents, unreacted amino acids and by-products remain in solvent. In all washing steps, this impurity containing liquid phase is removed from solid part with suction evacuation and peptide is filtrated. This cycle isrepeated until last amino acid is coupled and then short peptide sequences arecleaved from solid resin by using an anhydrous acid reagent. Thanks to this stepwise cycle, amino acid elongation in the resin can be controlled. By this way, by-product formation is minimized, racemization is eliminated, and most importantly, reaction yield increases in each coupling reaction step,.

In SPPS, polystyrene resins are generally used for 'immobilized' peptide on the solid-phase. Wang Resins for carboxyl acid ended peptides, and Rink Amide resin for amide ended are the most preferred ones among them. (Figure 1.2) Rink Amide resin, and all other amino acids are used with 9-fluorenylmethoxycarbonyl (Fmoc) protecting group. Fmoc is a base labile protecting group. In SPPS, piperidine is used for deprotection of the Fmoc group before each coupling step Besides, side chains of amino acids should also be protected in order to prevent undesired elongation. These permanent-protecting groups must be stable till the end of peptide synthesis. Therefore, generally the acid-labile groups are preferred for side-chain protection, such as tert-Butyloxycarbonyl (BOC). While peptide is cleaved from resin, this protecting group is removed as well.

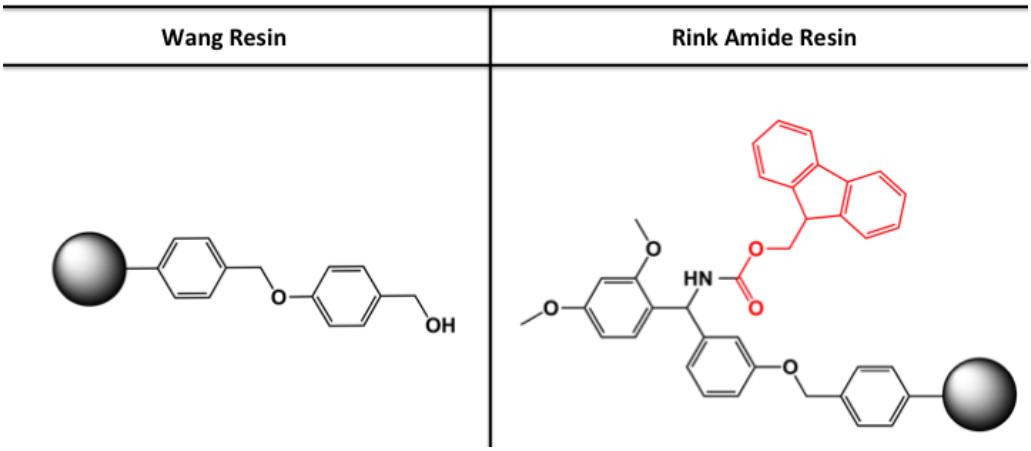

Figure 1.2 Wang resin and rink amide resin. Fmoc protecting group is shown in red color.

In addition to the resin, the solvents, which are used in the synthesis, have an important role in SPPS. There are two main solvents, which are used in the synthesis:dichloromethane (DCM) and N-N-dimethylformamide (DMF).(Figure-1.3) Both DCM and DMF are used in all washing steps. DCM is often used in swelling of polystyrene-based resins. Because it has a volatile feature and it is unreactive to TFA, peptide is collected with DCMin cleavage step.[7]All coupling reactions are performed in the DMF solution phase,since it has a fine polarity to dissolve all components of synthesis, including amino acids.

Coupling reagent is another important component of the solid phase peptide synthesis. Coupling reagents help to solve one of the main problems during peptide bond formation, which is called racemization. With the help of coupling reagents, enantiomerically pure peptides can be produced. There are several coupling reagents which can be utilized, such as HBTU, HATU, HCTU, and TBTU. (2-(1H-benzotriazol-1-yl)-1,1,3,3-tetramethyluronium hexafluorophosphate) HBTU is the most common one among them, which is used in coupling step (Figure-1.4). For coupling of amino acid, N,N-diisopropylethylamine (DIEA) is used with HBTU as an organic base for deprotonation of carboxyl group. (Figure-1.4). After each coupling step, free amines are checked by Kaiser Test. Even if Kaiser Test is negative, capping step is performed to ensure that there is no free amine left in the resin. Acetic anhydride is usedfor this purpose. (Figure 1.4)[8]

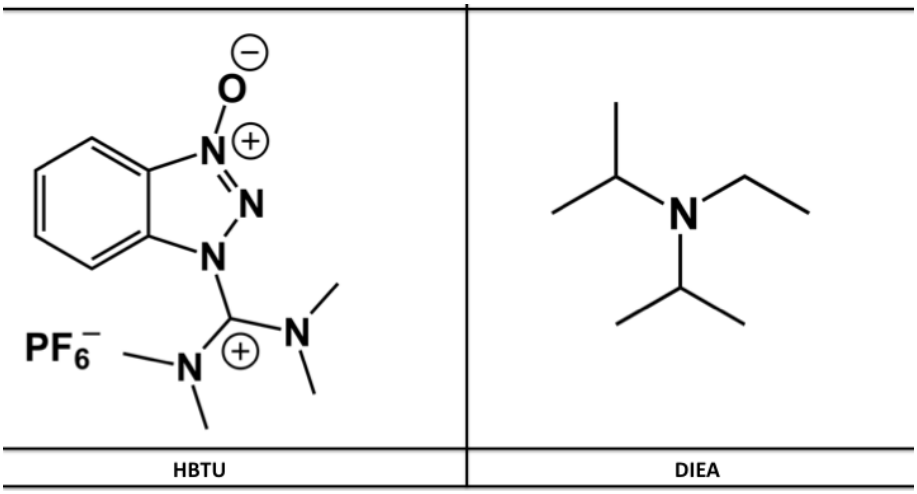

Figure 1.3 Coupling reagents

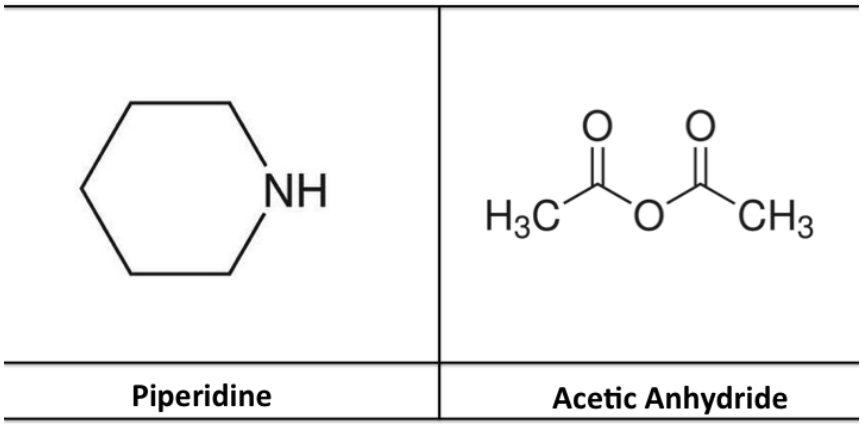

Figure 1.4 Base and free amine capping reagent

Final step of the SPPS is the resin cleavage. In this step, peptide is removed from resin by using a high concentrated strong acid, such as hyrdofloric acid (HF) or trifluoro acetic acid (TFA). Because of highly toxic feature of HF, it is generally not preferred. Therefore, utilization of TFA with anhydrous triisopropylsilane (TIS) as a scavenger is more common.

Trifluoroacetic Acid	Triisopropylsilane
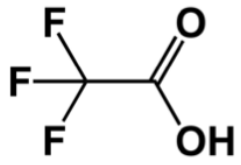	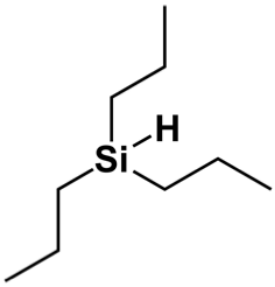

Figure 1.5 Peptide cleavage components

1.1.2 Reaction Mechanisms in the SPPS

Reaction steps are listed as protecting group cleavage, couplings and peptide cleavage in the previous sections. In this section, detailed mechanism will be explained. Each cycle starts with Fmoc protecting group cleavage. In all aminoacids purchased, Fmoc group was used to protect the amine side. Therefore, repeating cycles of reactions begin with activation of the first amino acid, which allows it to react with the second. This activation is obtained as a result of base-labile cleavage by mixing with20% by volume piperidine in DMF. Fmoc removal mechanism is initiated by protonation of piperidine (Scheme 1.1).This reaction produces unprotected amino acid and carbon dioxide.

Scheme 1.1 Fmoc protecting group cleavage by using piperidine

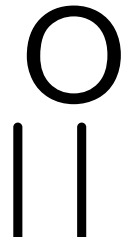

Scheme 1.2 Amino acid coupling mechanism

After first amine group of the first amino acid is deprotected, it is ready to form a peptide bond with the second one. Peptide bond is constructed between unprotected amine side of the first aminoacid, which is loaded on the resin and carboxyl side of the protected second amino acid. Amino acid coupling mechanism is depicted in scheme 1.2. Bond formation steps begin with deprotonation of second peptide's alpha-carboxylic acid in basic condition. Atthis step, DIEA is used as an organic base for deprotonation. Peptide bond formation is achieved by coupling reagent HBTU.

These two steps are repeated in each deprotection/coupling cycle till desired sequence is obtained. In the final step, peptide is removed from solid resin by mixing with 95% TFA. Same acid labile protocols are applied for both rink amide resin(scheme 1.3) andWang resin(scheme 1.4) . If there is a side chain protection, it is also unblocked in this strongly acidic condition. In order to prevent by-product formation due to carbocations, which forms as a result of deprotection of side-chains, so called scavenger TIS is used with TFA as well.

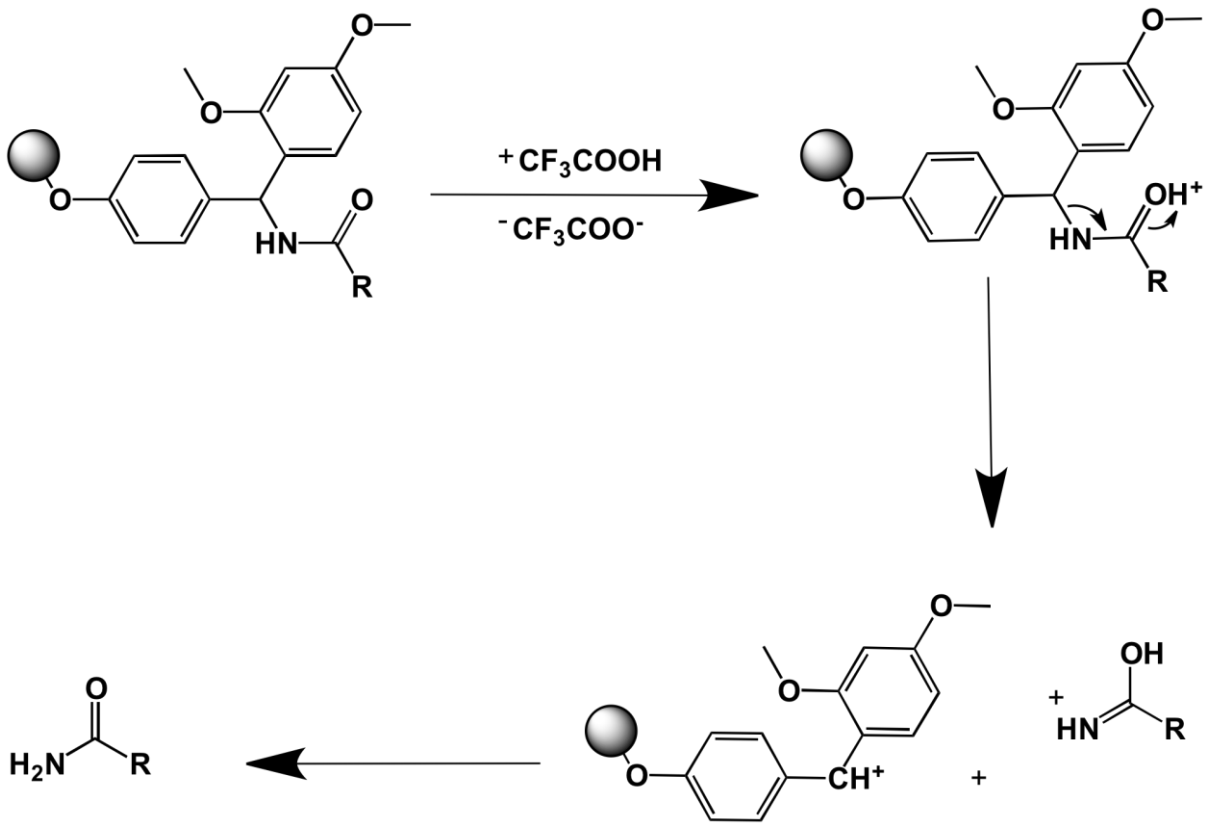

Scheme 1.3. Peptide cleavage from rink amide resin

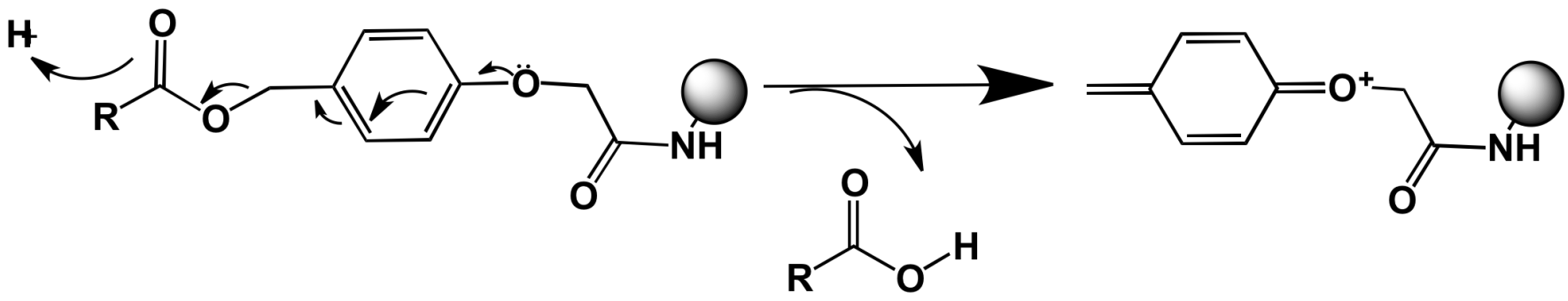

Scheme 1.4. Peptide cleavage from Wang resin

1.2. Self-Assembled Peptide Nanostructures

Self-assembly is both a natural process and a powerful bottom-up technique that spontaneously organizes chiral building blocks into well-ordered supramolecular nanostructures. Self-assembly is a spontaneous construction of building blocks through non-covalent interactions, such as hydrogen bonding, Van der Waals interaction, π-π stacking, hydrophobic interactions, electrostatic interactions, metal ion to ligand coordination [9,10]solvent effect and so forth.

Electrostatic interactions have essential roles in the self-assembly process. Coulombic interactions between building blocks can trigger self-assembly in a long range with 50-300 kJ/mole strength. However, these types of interactions are not selective. For example, in peptide amphiphile (PA) self-assembly, it occurs between two oppositely charged PA. [11]In neutral pH, two oppositely charged PAs co-assemble into nanofibersby charged neutralization.[12]Charged neutralization takes place as a result of strong repelling of the same charged species, and attraction of the oppositely charged building blocks in dynamic water environment.

Moreover, pH control also regulates the self-assembly due to electrostatic interaction. Increased pH triggers the self-assembly of positively charged peptide amphiphiles. This is reverse for negatively charged peptides which have a tendency to self-assemble into supramolecular structures in acidic pH.

Metal ion to ligand coordination is another common interaction, which is used in self-assembly. It is a directional interaction, which has a relatively shorter range with 50-200kJ/mole strength. Solvophobic interactions and π-π interactions are other short-range directional interactions. Among all other types of other interactions,π-π interaction is the weakest while covalent interaction is the strongest. Covalent interaction, which has almost 350 kJ/mole bond strength, is an irreversible interaction. So, this type of interactions isnot preferred in dynamic self-assembly systems. Another weak short-range interaction is van der Waals interaction, which is non-directional and non-selective inter molecular interaction.

Hydrogen bonding is one of the most abundant trigger forces in supramolecular organization, which effects folding and secondary structures of the proteins, polypeptides and short peptide sequences.[13]In Figure 1.6,structural organization of peptidesinto β-sheet and α-helix motifs is shown.[13]At this point, utilization of specific amino acid sequences determines the secondary structure of the supramolecules.[14]

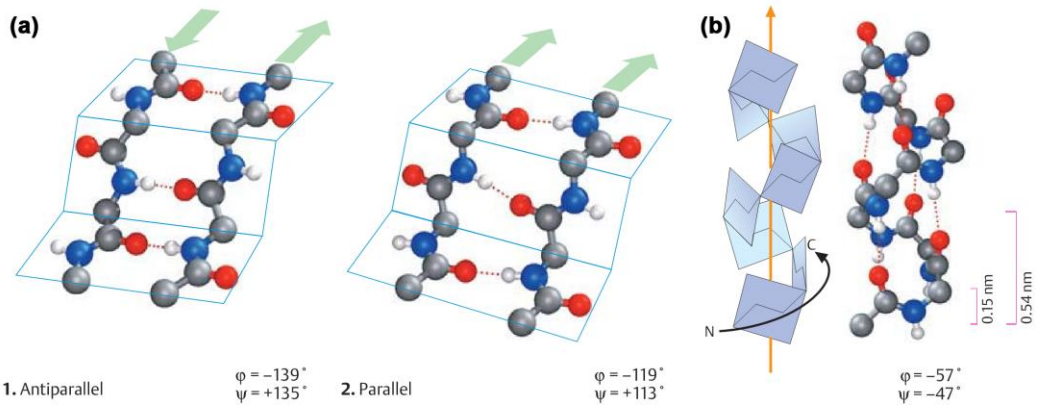

Figure 1.6H-bondingreproduced from Ref. [13] with permission from Thieme

All these noncovalent interactions play important roles to immobilize water or some other solvents encapsulated in self-assembled three dimensional network systems. Regulating these interactions make self assembly systems as excelent platforms to produce well-defined nanostructured soft materials like hydrogels. Adjusting size, shape, orientation and geometry atmolecular level with energy and energy free processes, results in better structural functionalization. Self-assembly is an easy fabrication method, by which larger morphological diversity can be obtained. Various types of nanostructures can be obtained in high amounts as a result of self-assembly, such as nanofiber structures,[14-18]nanotapes, nanobelts, nanotwists, [19-21]nanotubes, [22-25] nanospheres, [26, 27,28]hollow tubular structures, [24, 25,29, 30]andnanoflowers or cotton-like structures.

The environmental factors, which significantly influence the morphologies, can be stated as, aging time, temperature, photo-irradiation, ultrasonication, polarity, pH and ion concentration of solvent polarity. In addition to external factors, different types of building block molecules can also determine the final morphology as a result of different packaging. (Figure1.7)

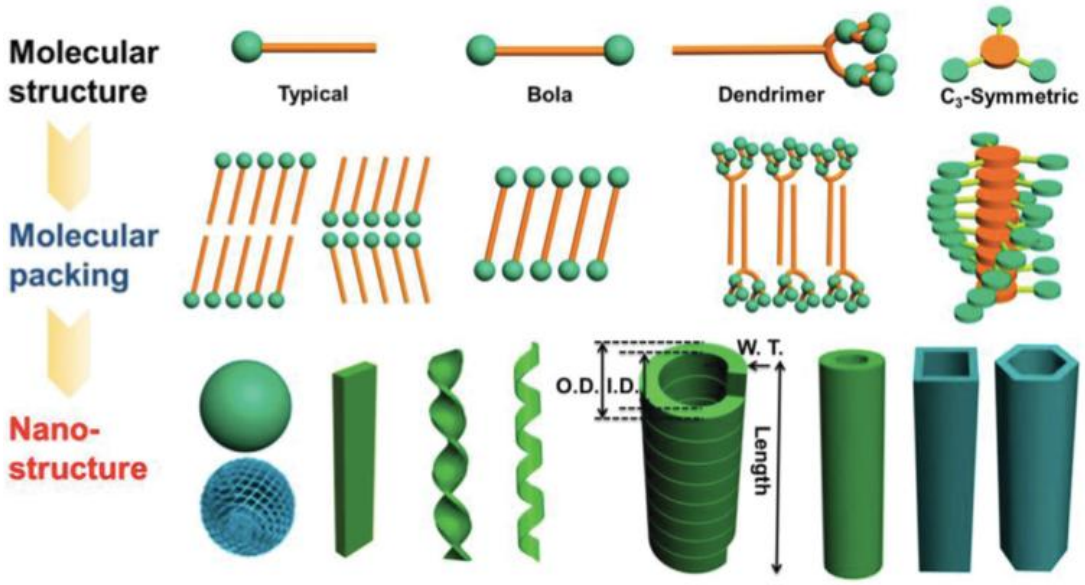

Figure 1.7. Various molecular packing ways of different building blocks**(**Reproduced from Ref. [75] with permission fromJohnWiley&SonsLtd)

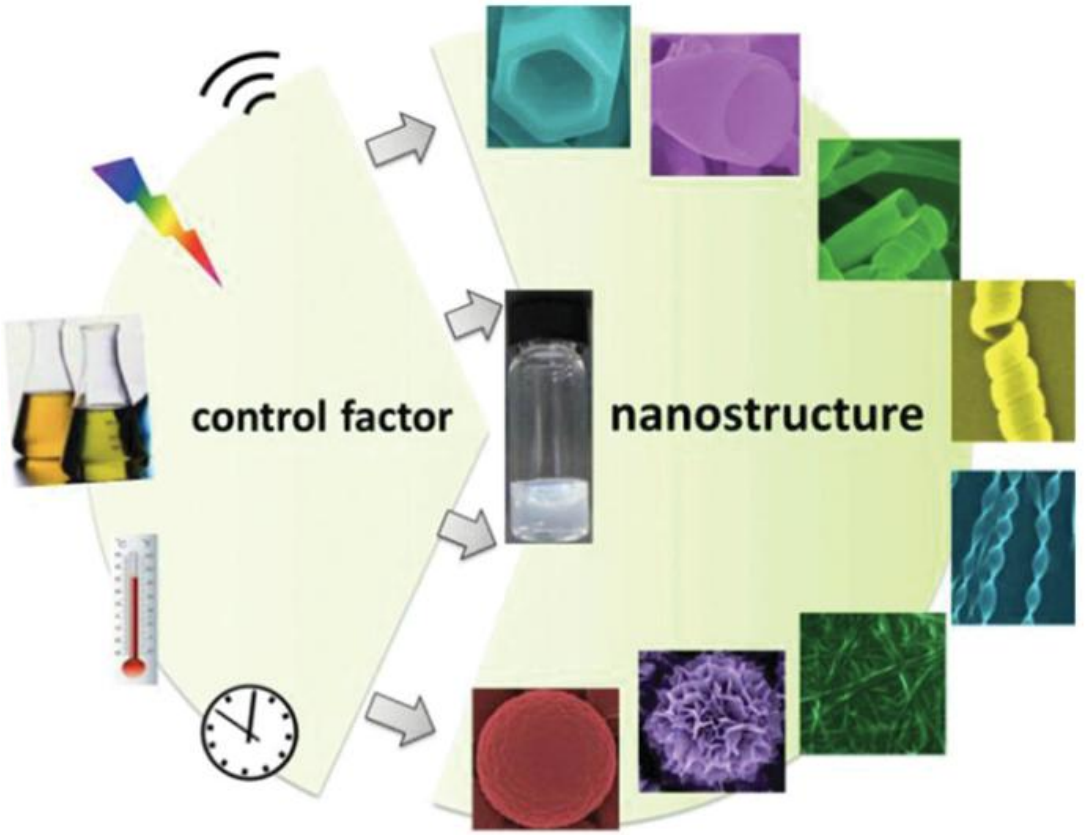

Figure 1.8. Morphological diversityof supramolecular nanostructures**(**Reproduced from Ref. [73] with permission fromJohnWiley&SonsLtd)

When elemental units hierarchically self-assemble in to complex structures, it is important to know how these building blocks come together. Assembly orientation of different types of self-assembly molecules affect to the final shape of supramolecules. Initial monolayer or bilayer structure formation is determinative for final morphology. For example, bolamphiphile molecules form a monolayer structure, and then they transform into nanotubes with single molecular wall thickness.[31]Amphiphilic molecules can initially stack as bilayer form, then form twisted or straight nanofibers, nanovesicles. On the other hand, multi bilayers produce nanobelts, nanotwists or helical nanoribbons. Some interesting shapes like hexagonal nanotubescan be obtained by using C_3-symmetrical molecular building blocks.[32]Among different kinds of gelator molecules, peptide amphiphile has been used as building block, due to their biocompatible, biodegradable, inert and functional properties. Peptide self assembly mechanism is illustrated in Figure-1.9. Typical peptide sequence consists of four major regions including hydrophobic region, hydrophilic region, β-sheet forming region and bioactive epitope. These regions are modified for desired chemical and biological functionality. Thanks to strong amphiphilic character of the peptides, building blocks organize in aqueous media as a nanofiber nanostructure. Entropic equilibrium is gained[58] when hydrophobic part of the peptides are buried inside the fibers and hydrophilic part of peptide locate on the fiber periphery of the sequences.

This supramolecular ordering of the peptide amphiphile molecules is robustly promoted by increasing hydrophobic character of molecules by adding any fatty acid residue to the sequence.[33]The fatty acid generally constructs the alkyl tail of the peptide amphiphile. The design is shown in Figure-1.13, lauric acid alkyl group was used as a hydrophobic moiety. Between hydrophilic and hydrophobic part of the amphiphile, specificmoiety is located which able to form inter molecular hydrogen bonding. Generally valine amino acid is preferred due its strong propensity of forming β-sheets secondary structure. This β-sheets forming region trigger the molecular packing in the favor of cylindrical geometry which allows engineering of various types of bioactive epitope on the fiber periphery.

The peptide amphiphile self-assembly is important for producing functional materials, and bioactive architectures. Peptide amphiphile nanostructures and particularly nanofibers, which has hydrophilic shell and hydrophobic core, are effectively used in encapsulation of the hydrophobic small molecules such as drugs [34]semiconducting molecules [35],carbon nanotubes [36] in aqueous media. The noncovalent functionalization of nanofibers enables producing electronically and biologically active hydrogel matrices, which ease the transduction of biological signals. Obtaining this functionality in physiological media opens the gates of biomimetic usage of peptide amphiphile in the regenerative medicine. Hydrogels consisting of peptide amphiphile network in water can act as artificial Extracellular matrices (ECM) [37]. The peptide amphiphile in hydrogel matrices, not only provide signaling between cells receptors and scaffold, but also provide mechanical and structural support to the seeding cells. This matrix can be tailored by changing bioactive epitope of peptide amphiphile depending on the desired application. For example, laminin- derivative IKVAV sequences are utilized for neurogenesis of neural progenitor cell[38] RGDS for hard tissue regeneration and replacement like bone tissue and bone marrow [40] and VEGEF for angiogenesis[41,42] Thereby, application of peptide amphiphile nanofibers was shown in literature with a great number of in vitro and in vivo studies.

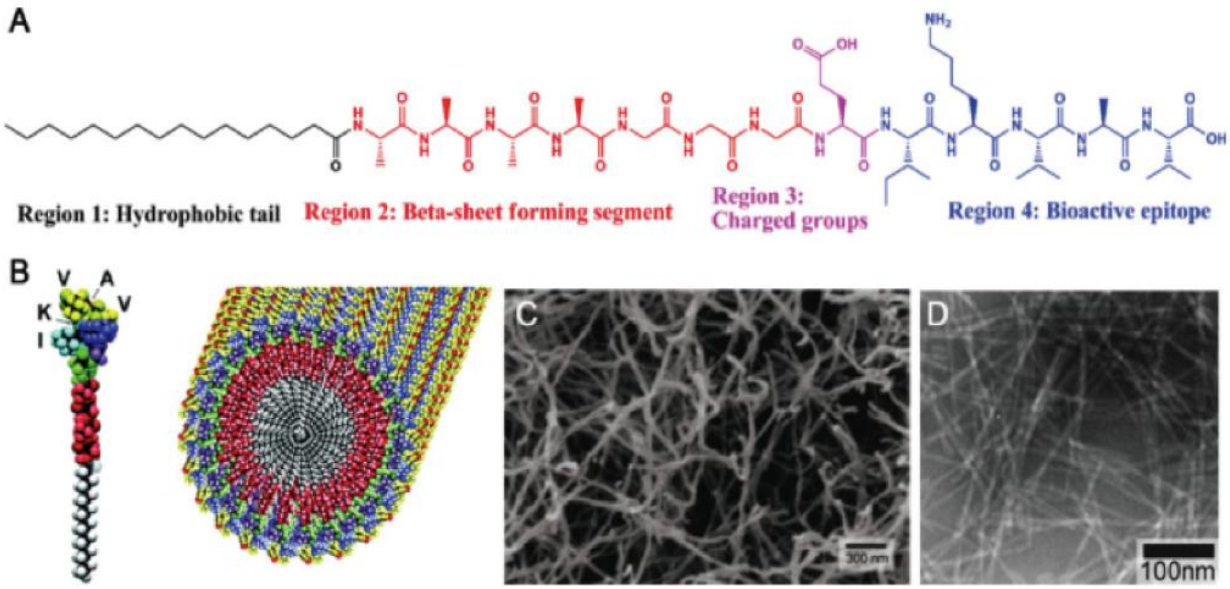

Figure 1.9. Self-Assembly mechanism of peptide amphiphile molecules blocks**(**Reproduced from Ref. [37] with permission fromAmerican Chemical Society)

Self-assembly occur not only among single type of monomer, but also in the mixture of different kind of building molecule co-assemble into higher aspect ratio supramolecules. These building blocks may either be oppositely charged molecule such as glutamic acid and lysine sequences contain peptides[13, 43]or enantiomers, which has reverse chirality. In a part of this research, co-assembly of the oppositely chiral L-PA and D-PA mixtures have been studied. It was reported in literature that, mixing of chiral building blocks show different morphology and handedness.Mixing chiral enantiomers has some draw backs, such as phase separation and heterochiral co-assembly, which means that aggregation of same chiral substances with each other. In other to obtain homochiral co-assembly, enantiomers are first mixed in a solvent, which building blocks totally disassemble in it. In our study HFIP (hexafluoroisopropanol) has been used. Later, it will be discussed in detail. [44]

There are several examples of chiral mixture study reported in literature. Earlier, Würthner and coworkers studied the perylene bisimide (PBIs) assemblies.In their study, reverse chiral PBI molecules containing oligoethylene glycol bridges was synthesized, and enantiomers co-assemble into supramolecular structures which has different handedness. Investigation results that; the co-assembly of chiral mixture system tends to produce homochiral aggregates.

Self-assembly of racemic mixtures are interesting new tools to develop stronger novel functional soft materials. Schneider and coworkers showed the improvement of the mechanical properties of peptide hydrogels by racemic peptide self-assembly. When mechanical properties of the gels prepared with β-hairpins racemic mixture was compared with hydrogels prepared from single type of enantiomer, racemic mixture displayed non-additive, synergistic improvement in the rigidity of soft material. They demonstrate enhancement in the macroscopic properties of soft matter by using rheological measurement.[45]

In another study, Wang et al. reported the co-assembly of the glutamicacid moeity containing bolaamphiphile (HDGA) racemic mixture with melamine. In this co-assembledsystem of the melamine with pure racemic, HDGA does not produce hydrogels. The assembly of HDGA racemate was precipitated. Mixing the HDGA

racamate with melamine formed well supramolecular gels. Bizarrely, the racemic gels enhanced mechanical rigidity. The gel forming ability, supramolecular chirality and nanostructures, which obtained after the assembly can be ordered by changing molar ratios of molecular building blocks. [46]

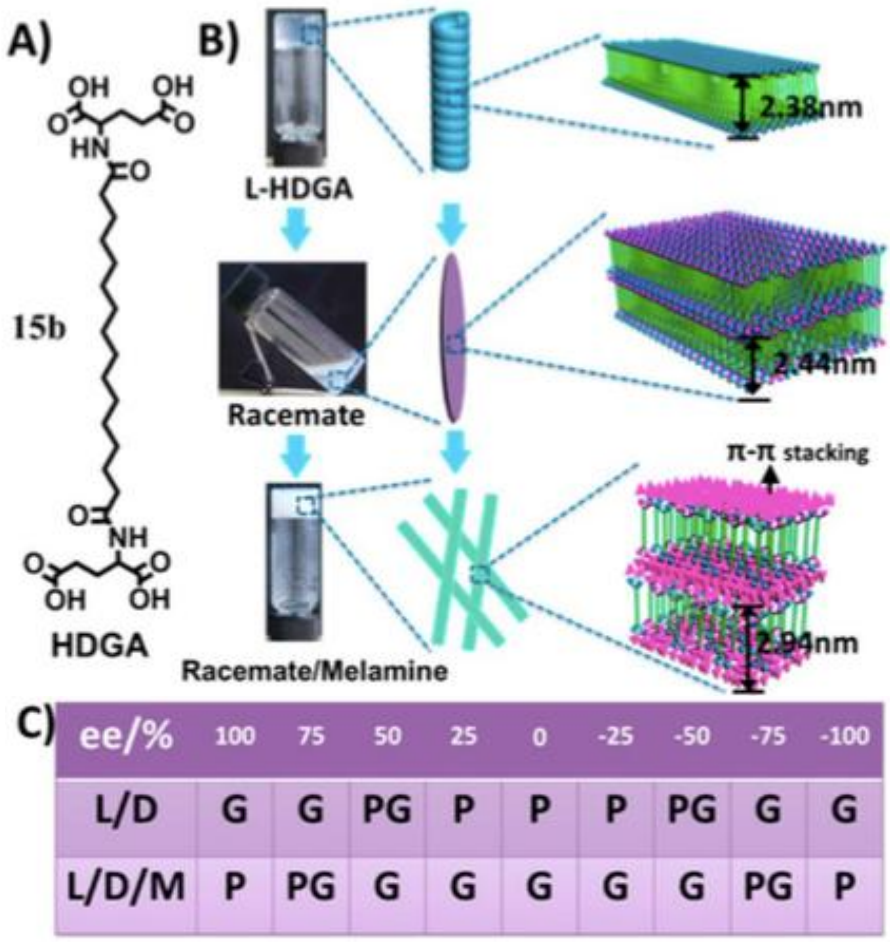

ee/%	100	75	50	25	0	-25	-50	-75	-100
L/D	G	G	PG	P	P	P	PG	G	G
L/D/M	P	PG	G	G	G	G	G	PG	P

Figure 1.10. Co-assembly of HDGA racamateblocks**(**Reproduced from Ref. 46 with permission fromAmerican Chemical Society)

In addition to gel forming ability and enhancement of the macroscopic properties of soft material, mixing of enantiomers has been used to tune the morphology of the diverse supramolecular assemblies. Oda and his coworkers reported the twists and nanotubes formed from the co-assembly of achiral dicationic n- 2-n Gemini type amphiphiles. They investigated that varying the enantiomeric excess of tartrate anions can continuously modulate morphologies of the coassemblies, such as the

twist pitch of the nanoribbons. For example, when 10 mole % of the opposite enantiomer of anions cause an increase of 15% in the diameter of nanotubes.[47]

In another research, Liu and his coworker synthesized L or D enantiomers of the glutamic-acid containing lipids. They investigated the co-assembly mechanism of the chiral enantiomers. L and D enantiomer of the molecules distinctively co-assembled into long nanotubes, however when D- and L- enantiomers mixing with different molar ratios, morphology changed consecutively from helical nanotubes to nano twists and then turn to flat nanoplates[48]. As a result, all those examples from literature show that, mixing enantiomer of chiral molecular building blocks provide interesting new tool for designing and developing powerful, novel functional soft materials.

1.3. Chirality and Supramolecular Chiral Nanostructures

1.3.1 Molecular and Supramolecular Chirality

Over the past decade chiral molecules attracted the interest of the researchers due to their superior optical properties. Chirality is essential property for designing chiral catalyst, biosensor and so on. Moreover, these molecules have potential application in the field of enantioselective separation, non-linear optics and manufacturing of circular polarizers.

Chirality term is used to describe the various scale objects, from subatomic particles up to galactic scale. [49] Between subatomic left-handed helical neutrinos and light-year scaled chiral galaxy system, there are a enormous number of chiral molecules exist. These enantiomeric molecules are listed as, nanoscale biomacromolecules such asDNA or proteins, self-assembled supramolecular structures, different kinds of microorganisms like helical viruses, tobacco mosaic, bacteria, macroscopic living systems like seashells, snails or plants can exist. Among these stages of chirality, molecular and supramolecular level chirality is attractive phenomena because it is strongly related to multidisciplinary research such as chemistry, physics, biology, medicine materials, and Nano-science. Moreover molecular and supramolecular chiral design of drugs and functional molecules promise a myriad of useful medical applications.

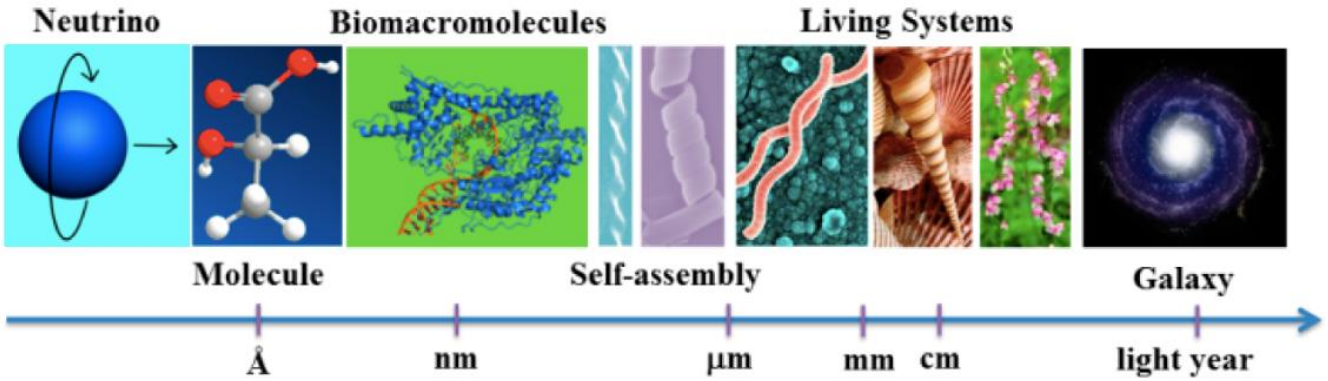

Figure 1.11. Chirality subatomic scale to macroscopic scale. reproduced from Ref. [57] with permission fromAmerican Chemical Society

Chirality in molecular level can be essentially categorized as point, plane, and axis chirality. Basically, the term of chirality is the description of objects that do not superposed with their mirror images. If a molecule is not superimposed with mirror image, then these molecules are called as chiral molecules. In practice, when deciding whether a molecule is chiral or not some shortcut methods are used. Generally finding out an asymmetric carbon atom, which four different atomic groups were attached on it, is easy way of determine the chirality of the molecules. The number of four different moieties comes from the sp3 hybridization of the carbon atom hybridization that enables the carbon form four covalent bonding in a molecule. Furthermore, there two more types of molecular level chirality, named termed planar chirality and axial chirality. Termed planar chirality observed when a molecule has more than one noncoplanar ring, which are dissymmetrically connected and does not simply rotate the chemical bond that connects them. Besides, if a molecule, which possesses an axis, that arranged of substituents is located in a spatial organization that is not superimposable on their mirror image. These molecules also accept as cihral even though there is lacks an asymmetric carbon atom. This is how chiral molecules differ in molecular level.

Chiral molecules possess both left and right type of handedness. According to this difference, specific type of isomerism is obtained called enantiomerism. In enantiomers, there should be at least one chiral center and four different atomic groups supposed to be attached this chiral center. Priority order of these attached groups helps to recognize the molecules handedness. If priority orders of groups are arranged in clockwise direction, the molecule is designated as (R). On the other hand if direction is counterclockwise enantiomer called as (S).

Figure 1.12. Molecular chirality and R/S system

Enantiomers generally show identical physical properties with their mirror image pairs. These pairs show different behaviors only when they interact with other chiral substances. For example, they can effect to the reaction rate and the enantiomeric excess of reaction product. Chiral molecules are optically active compounds. This most important feature of chiral molecules, which helps to separate different enantiomer with the help of rotating plane polarized light.

Chirality played an important role in evolution of living matter. For example, most important elements of the living organism such as DNA, RNA, proteins,and enzymes are consisted of chiral building blocks. L-amino acids are naturally selected as the essential component of proteins and enzymes; D- sugars are essential component of DNA and RNA. DNA is the most known chiral molecules, which possess right, handed double helix. R, S nomenclature of molecular chirality changed in amino acid naming as L for left handed amino acids, and D for right handed amino acids. In nature, amino acids exist in both L and D, except glycine. Glycine is achiral molecule because it has no side chain moiety.

Supramolecular chirality is directly related with the chemistry of entities produced by intermolecular noncovalent interactions which are explained detail in the beginning of the section. Supramolecular systems are strongly correlated to self-assembly that was described as the autonomous organization of small building blocks into higher aspect ratio structures without any external human intervention. This nano to micrometer sized architectures play an essential role in biological

systems. Transferring and storage of inherent information in nucleic acids is established by self-assembly feature in the biological systems, thanks to the folding ability of proteins into well-organized molecular machines. Supramolecular chirality is one of the consequences of biological molecular self-assembly.

There are several examples of the secondary configuration of the protein folding. These structures of proteins obtained can show a variety of conformations for example α-helix, β-sheet, and random coil secondary structures that display different supramolecular chiral feature. Supramolecular self-chiral assembly process bases on special three-dimensional arrangements of building blocks in the space. Even if chirality term sound like only related to the atomic and molecular organization of components in side of the molecule, supramolecular chirality cover the higher aspect chiral organization of not only chiral molecules, but also achiral components and the combination of chiral and achiral molecules. Besides, to assemble chiral molecules, creating achiral molecules or chiral supramolecular structures, is an attractive consideration for researchers. These interesting approach supramolecular chiral systems deepen the curiosity about explanation behind the supramolecular chirality. Further understanding of chiral behavior of the molecular assemblies in the supramolecular level will lighten the biological systems. Better understanding of chiral assemblies in living organisms, promisingly will assist innovations of new drugs and materials.

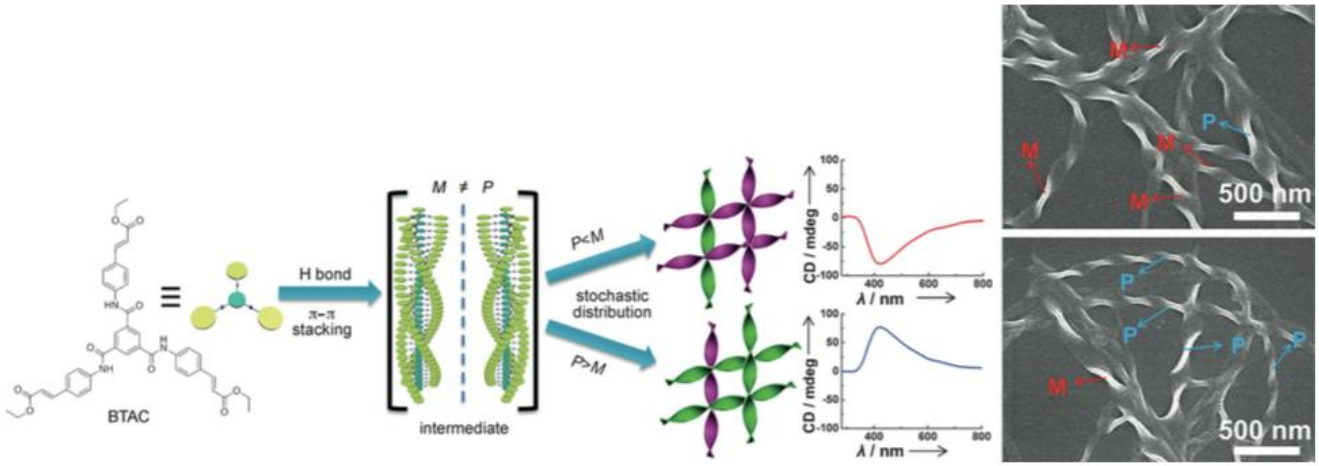

Figure 1.13.. Gelation process of BTACT**.** Reprinted with permission from ref [46]. Copyright 2014 John Wiley & Sons

In supramolecular level, nonsymmetrical organization of molecules through a non-covalent bond differ by handedness of the supramolecules. The traditional R, S nomenclature is changed as P, M naming the supramolecular construction. P naming is used for describing right-handed supramolecules, and M naming for left handed formation of building blocks.

In the recent study ofLiu and coworkers, they have investigated the synthesis of an achiral molecule, C3-symmetric benzene-1,3,5-tricarboxamide substituted with ethyl cinnamate (BTAC).[46]Moreover, they studied supramolecular gelation process of BTACT and its supramolecular chirality. They established that upon gel formation achiral compounds can simultaneously and autonomously produce unequal amounts of right-handed and left-handed twists (Figure 1.13)[46] . This macroscopic chirality of right handed and left handed twist has been confirmed by scanning electron microscopy (SEM) and circular dichroism (CD).They investigated that in each hierarchical self-assembly of BTAC molecule, system produce different morphologies and different cotton effect in the circular dichroism due to the unbalanced amount of right and left handed twists. When they examined the SEM image, both left-handed (M) and right-handed (P) twists are found in same sample. They concluded the results that obtained from of both SEM and CD as the right handed P amount is higher than left handed M, positive Cotton Effect was observed in the CD. In the opposite case, Right Handed P amount lower than Left Handed M Negative cotton effect was obtained. [46] (Figure-1.13.)

1.3.2 Chiral Amplification

Chiral amplification refers to increase the magnitude of cotton effect in the supramolecular system. In recent decades, attention to the chiral amplification has been increasing in the research of non-covalent interactions bade supra-molecular systems. In the supra-molecular assemblies, amplification of the chirality has been defined as an issue where local chirality of a small segment of chiral bias determines the chiral behavior of the entire supramolecular assembly. Generally, this

magnification followed by manifestation in cotton effect of the circular dichroism (CD) signals. [51-54]

One of the most famous study of this phenomenon reported by Green et. al. [55] In this pioneering study, they investigated poly-alkylisocyanates system, that influence the amplification of chirality. These influences called as “sergeants and soldiers” principle and the “majority rules”.

In the Sergeants-and-soldiers principle, (supramolecular) copolymerization of an achiral monomer with a small amount of homochiral monomer leads to a strong bias towards the macromolecular helicity corresponding to the chiral enantiomer.[56]As for Majority-rules principle, (supramolecular) copolymerization in mixtures of two enantiomers using a slight excess of one enantiomer leads to a strong chiral magnification in the overall supramolecular assembly.

1.3.3 Supramolecular Chiral Peptide Nanostructures

Supramolecular constructions are important chiral structures which has large potential applications based on chiral recognition, chiral sensing, [57] due to adjustable size shape and bioactive architectures.[58]

To understand the biological importance of supramolecular chiral peptide nanostructures, supramolecular chirality effects on cell behavior will be discussed. It is known from literature that, supramolecular peptide hydrogels that is produced by self-assembly of L-peptides and D-peptides, have compatibility with fibroblast cell in neutral pH. [59] Molecular level chiral differences in amino acid sequences effect to cell behavior such as viability and cell proliferation. Similar differences can be obtained in supramolecular level as well. In the study of Feng et. al., effect of handedness on cell adhesion was shown. (Figure 1.19) In this study, phenylalanine derivative peptide molecules was used as supramolecular fiber building blocks and it was obtained that, left-handed helical nanofibers increased cell adhesion and

proliferation. However, the right-handed nanofibers decrease cell adhesion and proliferation. Thus, they showed that cell behavior effects from chiral interaction between nanofiber and fibronectin. [60] In the same study, adhesion ability of two opposite supramolecular chiral nanostructures was compared. Opposite chirality was achieved by using amphiphilic L-glutamide and D- or L-pantolactone (LPGL, DPLG) enantiomers as a building block. Chiral nanostructures, which are formed from DPLG, show stronger adhesive ability to human serum albumin in vitro experiments. Moreover, this adhesion ability cannot be detected at the molecular level, it was only found after supramolecular chiral construction.

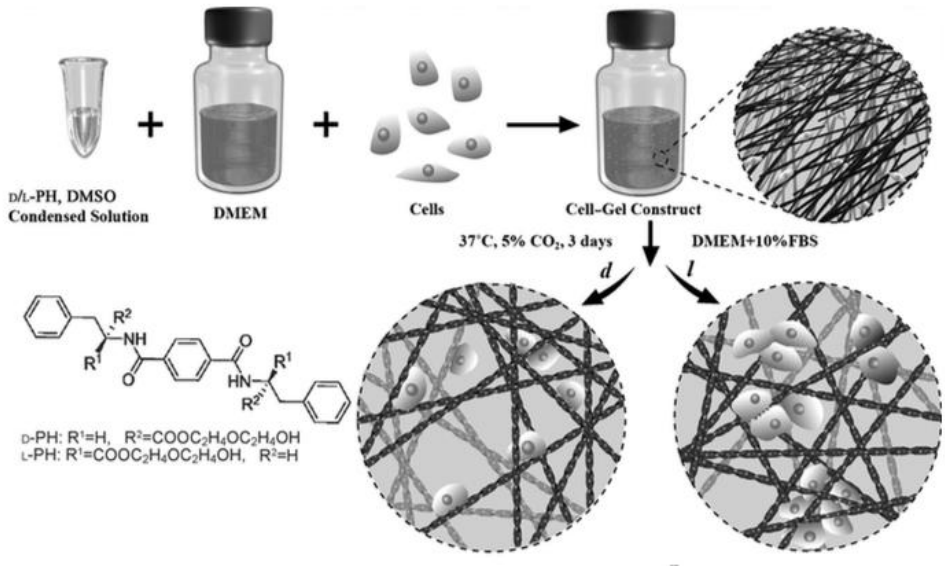

Figure 1.14. Effect of handedness on cell adhesion reproduced from Ref. 60 with permission fromJohnWiley&SonsLtd

However, differences in the morphology of the supramolecular structures are more significant than the handedness of molecules. For example, in the study of the Zouani and coworkers, it was found that human mesenchymal stem cell differentiation can be induced by different shapes and periodicity of the supramolecular chiral nanostructures.(figure1.14.) They produced, chiral silica

nanoribbons which support the human mesenchymal stem cell adhesion and differentiation and silica twists which is does not. [61]

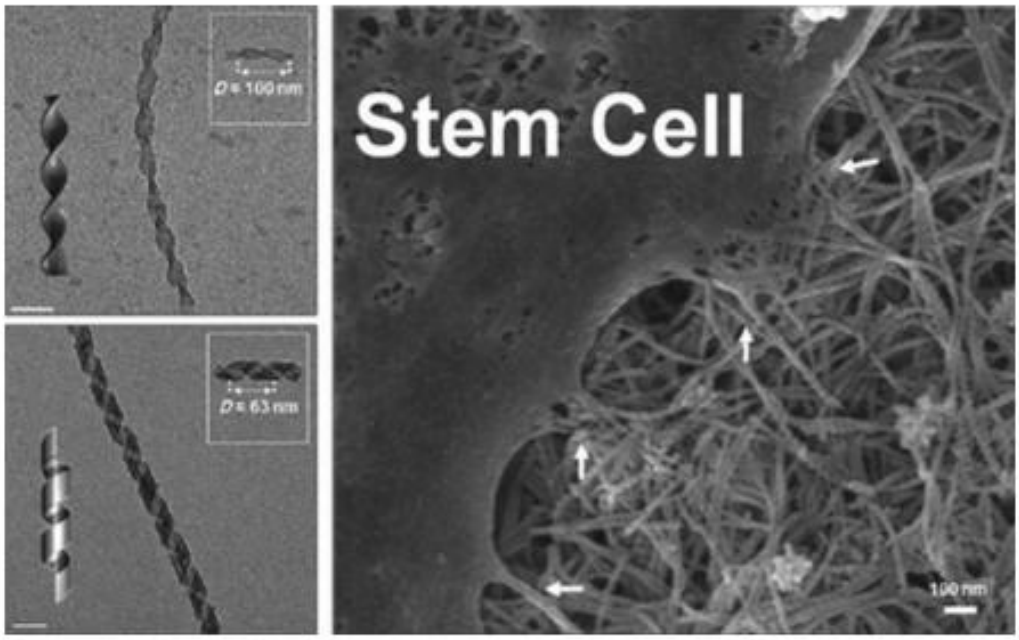

Figure 1.15. Human mesenchymal stem cell differentiation on chiral silica nanoribbons and silica twists. Reproduced from ref. 61 with permission from American Chemical Society

As a conclusion, supramolecular chirality is mainly dependent on the supramolecular chemistry manner of the molecular components. Usually, chiral molecules have the tendency to form particular chiral structures with defined supramolecular chirality. When chiral and achiral molecules are combined, achiral molecules might be induced into chiral construction deepening strong interaction between the achiral and chiral molecules in the self-assembly system. In Table-1, comparison between molecular and supramolecular chirality is listed. Both of them share some common characters and are strongly related. The supramolecular chirality concept cannot be understood without molecular chirality issue is considered.

Table 1.1. Supramolecular chirality

	Molecular Chirality	Supramolecular Chirality
Composition	**Atom**	**Molecule, Building Block**
Bond	**Covalent Bond**	**Noncovalent Bond**
Naming Convention	**R/S, L/D, M/P**	**M/P**
Chiral Geometry	**Tetrahedron, Axis, Plane**	**helical, spiral, chiral sheet, chiral domain**
Special Feature	**Point Axis, and Plane**	**conformation, secondary and tertiary structures, helicity etc.**
Manifestation of Chirality	**Fixed Chirality**	**Dynamic, Sergeant−Soldier Rule, Majority Rule, Chiral Memory**

1.4 Characterization of Peptide Amphiphile Nanostructures

1.4.1 Structural Analysis

After synthesizing peptides, the second important step of studying supramolecular self-assembly chiral peptide nanostructure is the characterization of the molecules. Before starting self-assembly experiment, peptides should be analyzed chemically and structurally. For this purpose, the Liquid Chromatography and Mass Spectrum (LC-MS) analysis is widely used. In the Liquid Chromatography part of the method, sample separation occurs according to retention time differences resulting polarity differences in mobile phase. In mass spectrum part, separated samples sensitively analyzed sample in the liquid phase according to flow rate of the charged molecules depending on their molecular weight.

1.4.2 Morphological Characterization

For characterization of peptides after the assembly, direct visualization of morphology by using highly advanced microscopic equipment is the basic technique. Here, mainstream method that is used in morphological characterization of the peptide amphiphile chiral images will be explained, and comparison between all these techniques will be provided.

Atomic Force Microscopy (AFM) is one of the common microscopic methods to understand nanostructures. The working principle of the method is based on the measurement the force between the tip and the surface of the sample. The sample is fixed on a piezoelectric scanner, which moves the sample under a tip mounted on a soft cantilever. As the sample passes under the tip, the force and interaction between the surface and the tip is measured, which produces an AFM image. AFM is used effectively to probe the surfaces at lower scale to the atomic level in air, vacuum, or other environments. The sample is commonly made up on a very flat surface, like silica or mica. For instance, in self assembly of L- glutamic acid or D-glutamic acid containing bola-amphiphile, assembled chiral nanotubes obtained by using AFM.[62]The major advantage of the AFM observation is that, the supra-molecular chirality of the nanotube can be directly judged. While L-glutamic acids containing bola- amphiphile produced a right handed helical nanotube, D-glutamic acids containing bola- amphiphile formed a left-handed one. [63]

Another important characterization technique is scanning tunneling microscopy (STM). This technology is based on quantum wave tunneling. The working principle of the STM relies on the flow of quantum tunneling current, resulting a voltage applied between the conducting tips. The gap between the tip and the surface determines the function of tunneling current. If the tunneling current kept constant by regulating the gap, the height of the surface can be outlined and then displayed as an STM image. This method provides an outstanding means for controlling the gap between the probe and the surface. Thanks to this method high resolution image of the samples can be obtained. For example it can directly discriminate the configuration of chiral object at a molecular level resolution. [64]

In addition to STM and AFM the scanning electron microscope (SEM) is another widely used microscope to examine the surface topographies of materials. The idea behind the SEM is the interaction of electrons with the atoms on the sample surface, and detecting the x-rays and electrons to understand the features of the surfaces.

SEM uses electron radiance to produce images by the reflected electrons. SEM is critical in different kind of fields which require the characterization of solid samples. Although scanning electron microscope displays images in sense of three

dimensions, results are taken as two dimensional photographs. Therefore, this method is especially beneficial for sensing chiral structures like helices or twists.

Similarly, transmission electron microscopy (TEM) is a common technique which provides two dimensional photographs of structures. In this microscopy method, a beam of electrons passing from ultrathin specimen interacts with the specimen. The interaction between sample and electrons which transmitted from more than 200nm thickness specimen form image in TEM. Beneficially TEM offers a very high resolution, which around the 0.1 nm scale. Therefore, it is useful to determine the morphology of nanomaterials. It is also advantageous to monitor chiral structures. For instance, by using TEM, in self-assembly systems, helical twist structure was constructed by a pyridine including amphiphilic L-glutamide. [65]

All of these techniques are effectively used in the observation of chiral nanostructures. However, this does not mean that all techniques are suitable for all samples. Among all of these methods, the proper one should be chosen depending on the features of the sample that used in the self-assembly systems. For example, for the self-assembled peptide amphiphile gel systems in this study, AFM and TEM were preferred due to their transparent gel-forming feature. Moreover, TEM provide fine monitoring scale instead of SEM for nanostructures that are investigated from peptide amphiphile self assembly.

1.4.3 Spectroscopic Characterization

In addition to direct visualization of chiral nanostructures, detecting chirality by using spectroscopic techniques helps to understand dynamic features of the supramolecular structures. Usually, spectroscopy techniques used for characterization of chirality in molecular level, can be used for detecting chirality in supramolecular level. There are several spectroscopic methods used for analyzing chiral structures such as linear dichroism (LD), circular dichroism (CD), vibrational circular dichroism (VCD), and circularly polarized luminescence (CPL), and so on. Among these methods, circular dichroism spectroscopy is the widely used one for characterization of chiral compound. Most powerful part of our study is based on circular dichroism measurement. Therefore, in this part, the details of CD method will be explained. Circular dichroism was developed to analysis of molecular chirality. Nevertheless, there are several examples provide detailed investigations of CD spectroscopy utilization in supra-molecular systems. It was found that, there are many reasons make this method specifically useful for monitoring self-assembly systems.

First of all, circular dichroism is very beneficial to obtain information depending on varying dynamics, which affects the fate of self-assembly, such as aging time and temperature. Because self-assembly is a dynamic system where disassembly and assembly simultaneously could occur, regulating external parameters during measurement is extremely important to obtain precise information.

Second, circular dichroism signals originate from the electronic transitions of the chiral molecules. This means that CD is un-sensitive to achiral molecules, and this method only detects the molecules which posses chiral sense or chiral packing. As stated in previous section, during the self assembly process, molecular packing plays most important role in the fate of chiral nanostructures. In this line, CD spectrum is essential since it provides detailed knowledge about packing of the supramolecules, and the secondary structures of the proteins.

Circular Dichroism (CD) is a powerful technique to detect the chiral characteristics of supramolecular systems. Especially, CD is widely used tool to study peptide conformations because it is very sensitive to peptide conformation and structural change. CD is often used to follow folding/unfolding transitions in globular proteins.The electronic transition of proteins depends on differential absorption of left versus right circularly polarized light, records as a function of wavelength in CD spectrum. Wavelength is divided into tree regions; the far UV region, which is below 250 nm wavelengths, aromatic region between 250nm-300nm, visible regions 300-700nm.

CD can obtain variety of different folding structure. Typical CD spectrum of most common secondary structures such as α-helix, β-sheet, random coil are listed in Figure 1.16

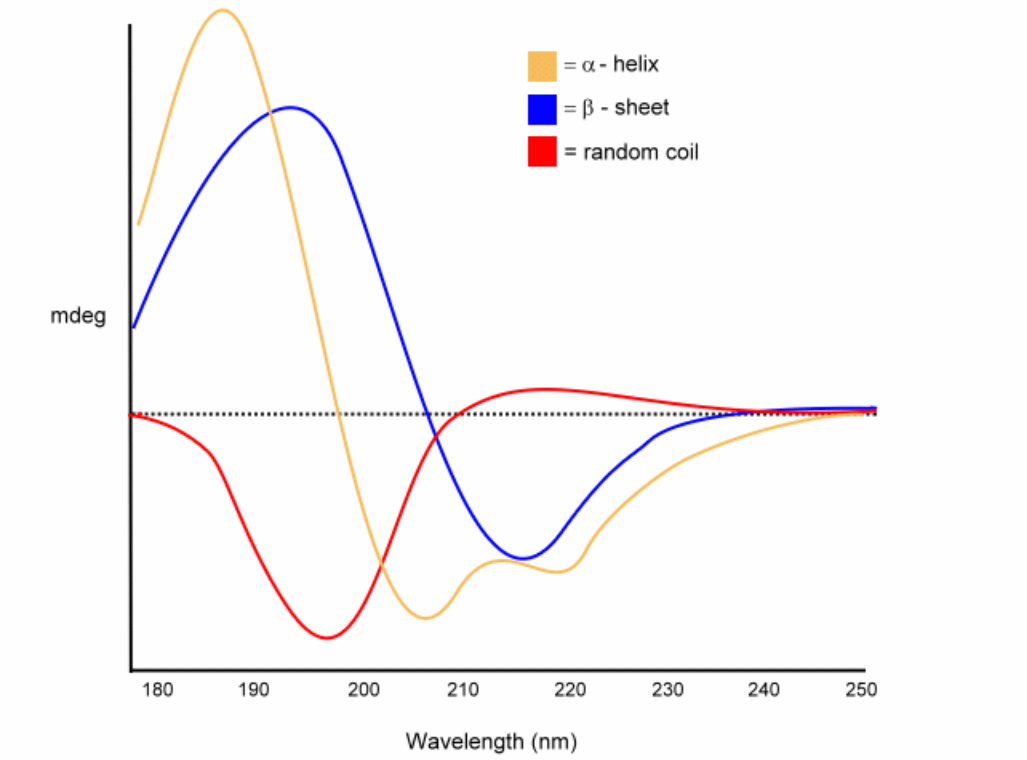

Figure 1.16.: α-helix, β-sheet, random coil CD signal

Secondary structure of the proteins originates from electronic transition between the amide and carbonyl bond. The intensity and energy of these transitions depends on the angles of the peptide bond. In previous studies of our research group, β-sheet forming tendency of the peptide amphiphile molecules was reported. [13, 43, 67] Therefore, β-sheet secondary structure will be discussed in the rest of section.

Typical β-sheet CD spectra is shown in figure-1.16. In L-peptide, the negative band in the 216 nm is due to the peptide nΠ* transition, and the positive band near 195 nm and negative band arise from the excitation splitting of the lowest peptide ΠΠ* transition. For D- peptide reverse signals are obtained, positive band in the 216 nm, negative band near 195 nm. [66,73]If amphiphile molecules assemble with 90^0 degree angle to the virtual axis, which is supposed to pass through the center of the fiber, a perfect c is formed. However, during self-assembly perfect β-sheet does not always produced. Sometimes building blocks come together with more than 90°degree angle, this rotation cause twisting β-sheet secondary structure. [68](Figure 1.22)

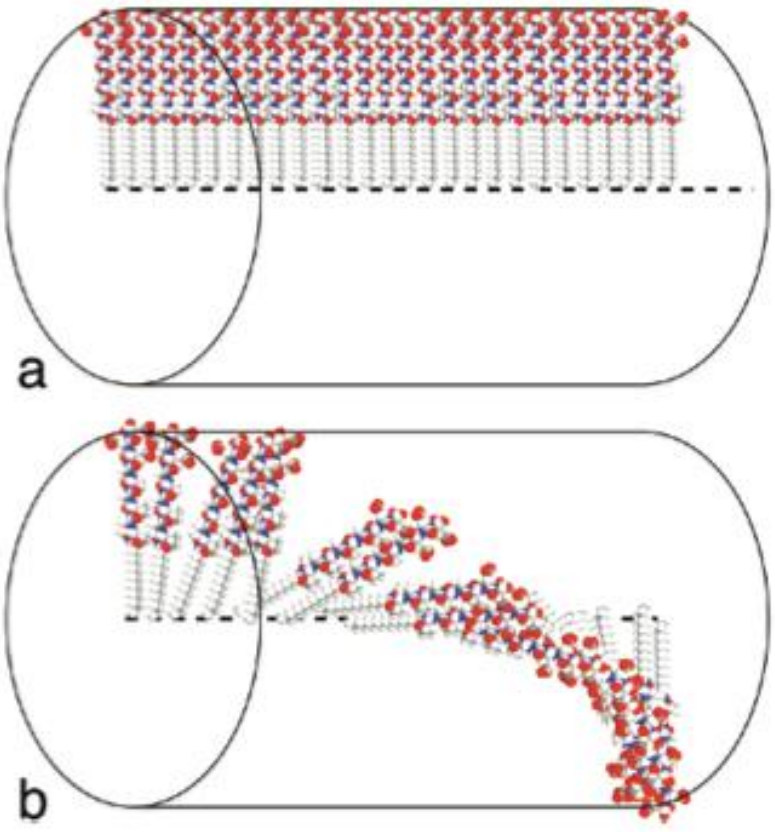

Figure 1.17. Twisted β-sheet in nanofiber. Reprinted from ref. [68] with permission from American Chemical Society

For example, Stupp and coworkers reported series of peptide amphiphile with modified β-sheet regions, and they observed the relationship between amino acid sequences and twisting structure. In this study, they investigated the twisting β-sheet by changing the position and number of the strong β-sheet forming amino acids valine, and weak β-sheet forming amino acids alanine. The degree of twisting can increase the entropy of the β-sheet. The twisting amount of the hydrogen bonding in the β sheet cause to increase in the length of bond which makes it weakened.[69, 70]Therefore, amounts of disorder in the β-sheet can be monitored by both red shift and intensity differences in circular dichroism spectra. (Figure-1.23)

Thus, CD spectra provide beneficial tools to understand chiral behaviors of the both molecular chirality and supramolecular chirality. Beside, CD spectrum can be

informative about the assembly mechanism of the building blocks depending intensity and wavelength of the CD signal.

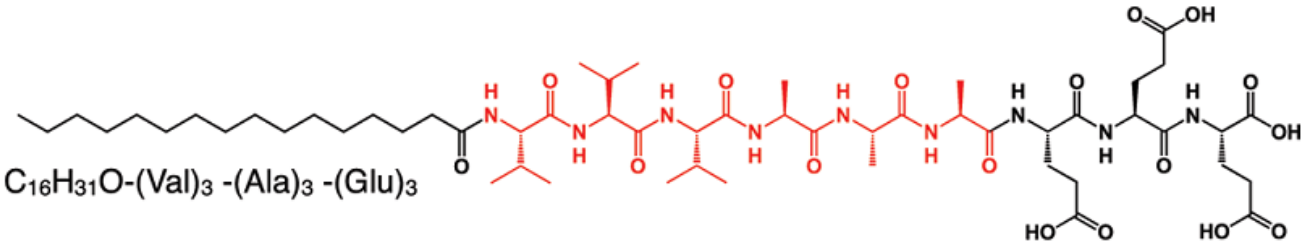

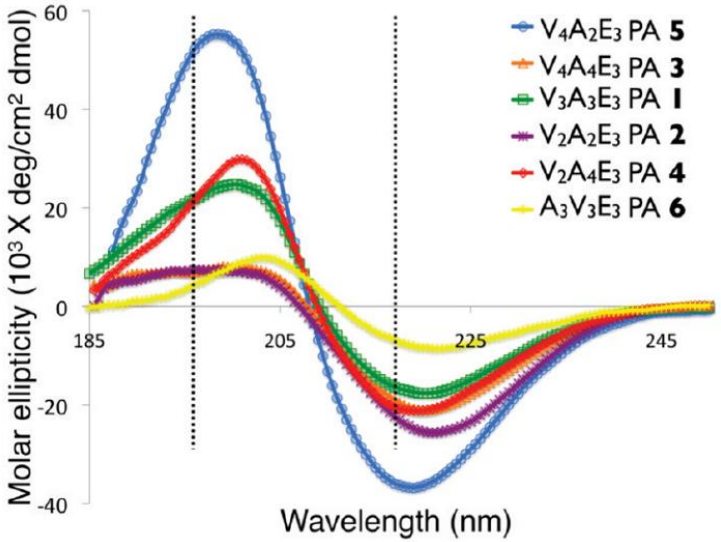

PA	β-sheet region
PA **1**	VVVAAA
PA **2**	VVAA
PA **3**	VVVVAAAA
PA **4**	VVAAAA
PA **5**	VVVVAA
PA **6**	AAAVVV

Figure 1.18. Chiral Signals of Twisted β-sheet in Circular Dichroism.Reprinted from ref. 68with permission from American Chemical Society

Chapter 2

2.1 Introduction

Chiral building blocks attract the great attention because of their high-class optical properties. Chirality is a vital property for designing biosensor[76]chiral organocatalyst.[77] Moreover, these molecules have potential application in the field of enantioselective separation, non linear optics and manufacturing of circular polarizers.[78] Self-assembly is a powerful bottom-up technique to design and synthesize dynamic complex structures at nanoscale with atomic control. Self-assembling molecules with different chemical and physical properties have been studied in different scientific disciplines and applications such as material science, bioengineering, regenerative medicine and drug delivery.[79] Self assembling peptide amphiphiles are synthesized by conjugating peptides to hydrophobic moieties, commonly fatty acids. Biocompatibility and bioactivity of self-assembled peptide nanostructures have been investigated in the literature and also in our studies.[13, 43]The recent advances show that these structures are suitable platforms for tissue regeneration, stem cell differentiation and regenerative medicine due to self-supporting and extracellular mimicking properties.[80] On the other hand, dynamic nature of self-assembled peptidenanostructures and molecular level effects on cellular behavior are still studied, and the effects of morphological and

supramolecular chirality differences of self-assembled nanostructures on biological responses are not well understood.

In this thesis, we aimed to study dynamic nature of self-assembled peptide nanostructures and how morphological and supramolecular chirality of self-assembled peptide nanostructures affects the biological responses. The self-assembly mechanism of peptide amphiphile molecules synthesized withdifferent chirality was studied. For this purpose, the self-assembling peptide amphiphile molecules with different amino acid sequences and similar self-assembling conditions will be synthesized at both D and L chirality. Also, amino acid sequence differences in the β-sheet region of peptide amphiphiles lead to self-assembled nanostructures with different morphologies at similar conditions.

These supramolecular chiral peptide nanostructures were studied in detail by different spectroscopic techniques and imaged by TEM, STEM and SEM. Utilized peptide sequenceswere purified by high pressure liquid chromatography (HPLC), characterized by circular dichroism and ultra-violet spectroscopy, and their mechanical properties were analyzed by oscillatory rheometry.

The important aspect of this study is to understand morphological differences of self-assembled peptide nanostructures due to chiral mixtures in the dynamic system and evaluate biological consequences of these complex nanostructures on cellular behaviors at the same content. In addition, the chiral complexity of the system will provide a new platform for building dynamic networks and components for biological applications, and will model the behavior of self-assemblies of supramolecular structures found in living organisms. Also, the study on cellular behavior and differentiation on chiral mixtures of self-assembled peptide nanostructures with different morphologies and complex systems will provide scientific knowledge and new insights for biological sciences and regenerative medicine.

2.2 Experimental

2.2.1 Materials

Fmoc and Boc protected amino acids, MBHA Rink Amide resin, and HBTU were purchased from NovaBiochem. All solvents include hexafluoroisopropanol was purchased from Sigma Aldrich.

2.2.2 Synthesis of Peptide Amphiphile by Using Solid Phase Peptide Synthesis

L-Lauryl-Val-Val-Ala-Glyl-Lys- (L-VVKK) , D-Lauryl-Val-Val-Ala-Gly-Lys-Lys (D-VVKK), L-Lauryl-Phe-Phe-Ala-Lys-Lys (L-FFKK), D-Lauryl-Phe-Phe-ALA-Lys-Lys (D-FFKK) , L-Lauryl-Val-Val-Ala-Glu-Glu (L-VVEE) , D-Lauryl-Val-Val-Ala-Glu-Glu (D-VVEE) , L-Lauryl-Phe-Phe-Ale-Glu-Glu (L-FFEE), D-Lauryl-Val-Val-Ala-Glu-Glu (D-FFEE), peptide sequences (Scheme-1) were synthesized by using standard Fmoc chemistry. All sequences including lauric acid tail were constructed on Fmoc-Rink Amide MBHA resin. Amino acid coupling reactions were performed with 2 equivalents of Fmoc-protected amino acid, 1.95 equivalents of HBTU and 3 equivalents of DIEA for 2 h. The Fmoc protecting group removal was performed with 20% piperidine/DMF solution for 25 min. Cleavage of the peptides from the resin was carried out with a mixture of TFA : TIS : H2O in a ratio of 95 : 2.5 : 2.5 for 2 h. Excess TFA was removed by rotary evaporation. The remaining peptide was triturated with ice-cold diethyl ether and the resulting white precipitate was freeze-dried. All peptides was purified by Preparative Liquid Chromatography (Prep-HPLC) and positive peptides were treated with 1mM HCl

2.2.3Sample Preparation

1% (weight) peptide solution was prepared in water. For basic samples, solution was gelified with 0.5 M 10 uL NaOH solution, for neutral samples, gel was prepared by mixing KK-PA and EE-PA.

For chiral mixtures, each peptide was first dissolved in H-bond donatingsolvent hexafluoroisopropanol (HFIP). First, peptides, which have different chirality,were mixed in HFIP with 100% 75% 50% 25% 0% ratio. All mixtures were dissolved in water after they were dried under vacuum and HFIP was removed thoroughly. Thanks to this procedure, self-assembly process start simultaneously for each building block. Moreover, mixing peptides in HFIP before assemble them in water, provides L and D form of peptides assemble together. Preparation Method, which is used in chiral mixtures, was represented in Figure-2.1.

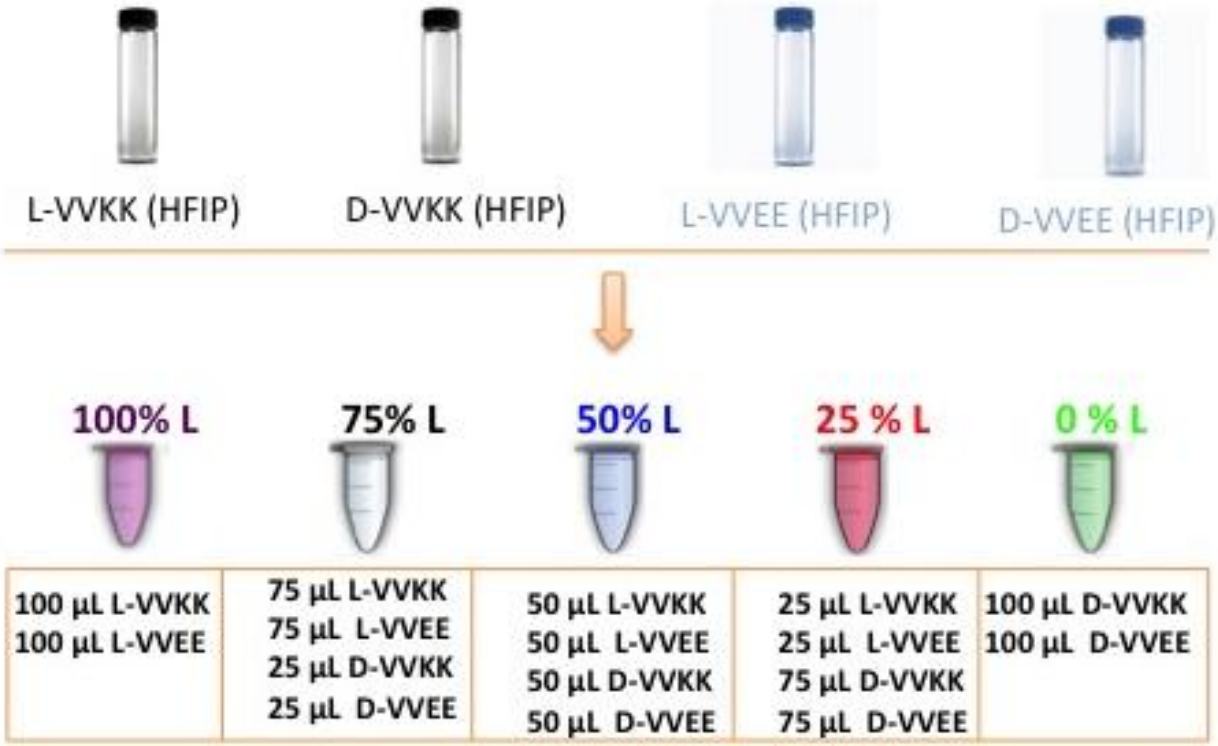

Figure 2.1 Chiral mixture sample preparation

2.2.4 Liquid Chromatography

For the structural and chemical analysis of the peptide, Agilent Technologies 6530 Accurate-Mass Q-TOF LC-MS with Zorbax SB-C8 column were used. Concentration of the sample for LC-MS measurement was 0.5 mg/mL. Solvents were water (0.1% formic acid) and acetonitrile (ACN) (0.1% formic acid). LC-MS was run for30 min for each sample and it started with 2% ACN and 98% H2O for 5 minutes. Then,gradient of ACN reached to 100% until 20 minutes. Finally, its concentration was dropped to 2% and it kept running for 5 min. Solvent flow was 0.65 mL/min and 5 µL sample was injected.

2.2.5 Circular Dichroism (CD)

A Jasco J-815 CD spectrophotometer was used for CD analysis. 1% (weight) peptide solution was prepared in water. It was gelled with 0.1 M 10 µL NaOH (for pH 6) 0.1 M 20 µL NaOH (for pH 8) and 1M 5 µL NaOH (for pH 10) and kept there over night.(pH was around 8) After peptide gelified well it diluted first 2mM concentration. Then by using this stock solution 0.25 mM circular dichroism sample prepared in 1mm Quartz Cell. Peptide solution was measured from 300 nm to 190 nm with 0.1 data pitch, 100 nm/min scanning speed, 1 nm bandwidth and 4 s D.I.T. Average of three measurements were used, and sensitivity was selected as standard.

2.2.6 Transmission Electron Microscopy(TEM)

Imaging of the peptides was achieved by TEM (FEI, Tecnai G2 F30) worked at 100 kV. For peptide amphiphile nanofiber staining, uranyl acetate solution in water (2 wt%) was used. 2mM stock solution was 40 times diluted. Diluted samples were placed on a Lacey carbon coated copper grid. 10 mL of diluted sample solution was dropped on a grid and kept there for 8 min. The excess was removed by pipette. Then, 20 mL of 2 wt% uranyl acetate solution was put on a parafilm sheet. The grid was placed on the top of the drop with its upper side down and kept there for 5 min. Stained grids were dried in the fume hood at room temperature overnight.

2.3 Results and Discussion

2.3.1 Building Blocks of The Chiral Self-Assembly

In this study, morphological diversity of chiral peptide was tuned by performingself-assembly in different pH values with different amino acid sequences. 12 different peptide amphiphiles were designed and synthesized.(Table-3.1). In hydrophobic part,lauric Acid was usedbecause it is long enough totrigger specific nanofiber organization in water. Hydrophobic part and hydrophilic part linked together by using valine-valine amino acid sequences which orchestrate in the favor of β-sheet secondary structure. Valine was chosen due to the highest propensity of forming β-sheet secondary structure.[20]For diversity of the morphology, valine-valine replaced with aromatic phenylalanine-phenylalanine moiety. The presence of a center π–π stacking in the peptide sequence was demonstrated to be an important factor in promoting the twisted nanofiber morphology and a stronger network. [73]On the other hand alanine is a weak β-sheet former, it was used as linker between hydrophobic and hydrophilic moiety. In hydrophilic part double lysine was preferred for positive peptides and double glutamic acid was chosen for negative peptides. Lysine was preferred due to the ability of forming hydrogel in water without addition of initiative substance.

Table 2.1. List of Peptide Amphiphile building blocks

L- PAs	KK	EE	HH
VV	Lauryl-VVAGKK (L-VVKK)	Lauryl-VVAGEE (L-VVEE)	Lauryl-VVAGHH (L-VVHH)
FF	Lauryl-FFAGKK (L-FFKK)	Lauryl-FFAGEE (L-FFEE)	Lauryl-FFAGEE (L-FFHH)
D-Pas	KK	EE	HH
VV	Lauryl-vvaGkk (D-VVKK)	Lauryl-vvaGee (D-VVEE)	Lauryl-vvaGee (D-VVHH)
FF	Lauryl-ffaGee (D-FFKK)	Lauryl-ffaGee (D-FFEE)	Lauryl-ffaGee (D-FFHH)

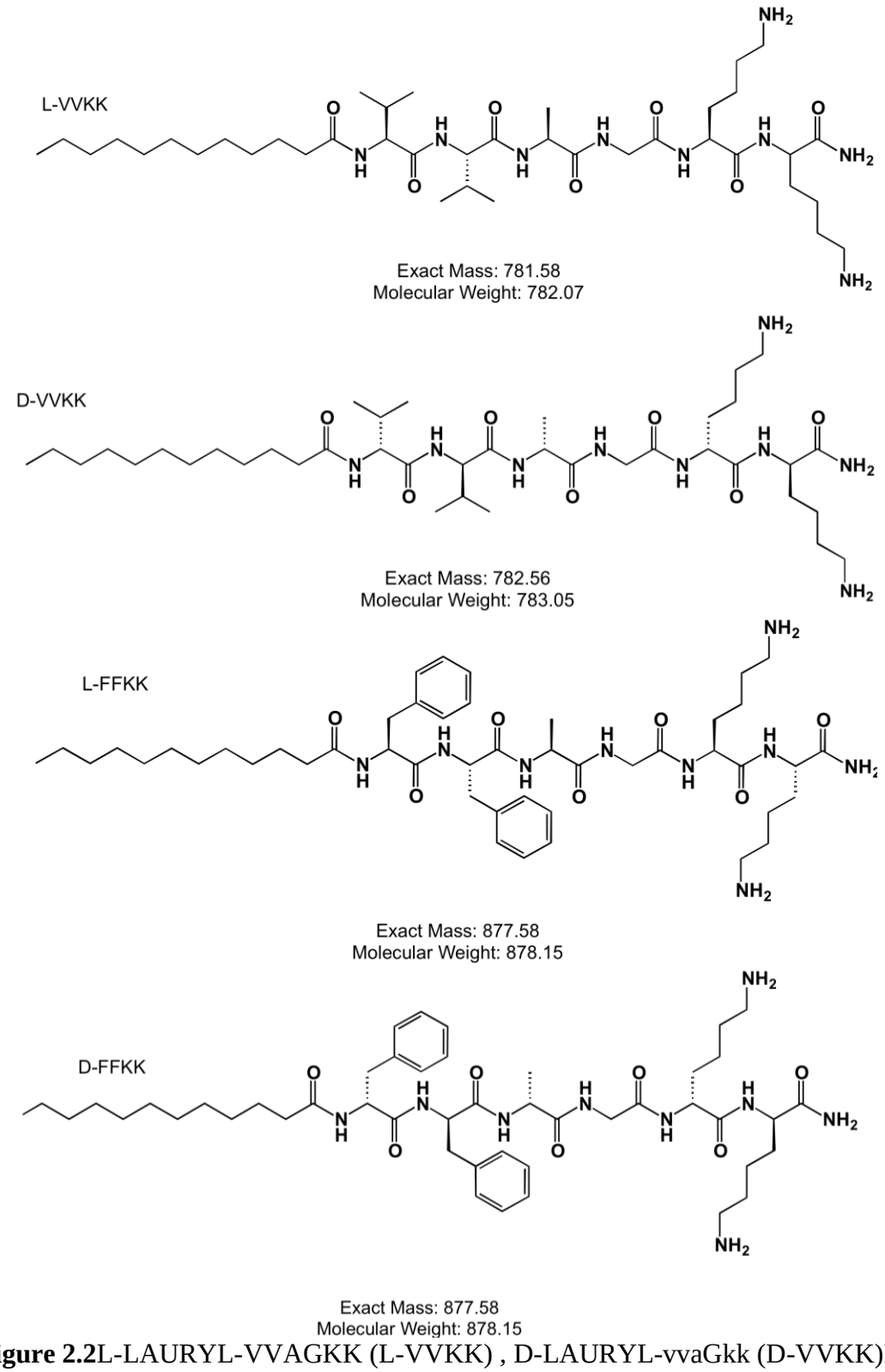

Figure 2.2L-LAURYL-VVAGKK (L-VVKK) , D-LAURYL-vvaGkk (D-VVKK)L-LAURYL-FFAGKK (L-FFKK), D-LAURYL-ffaGkk (D-FFKK)

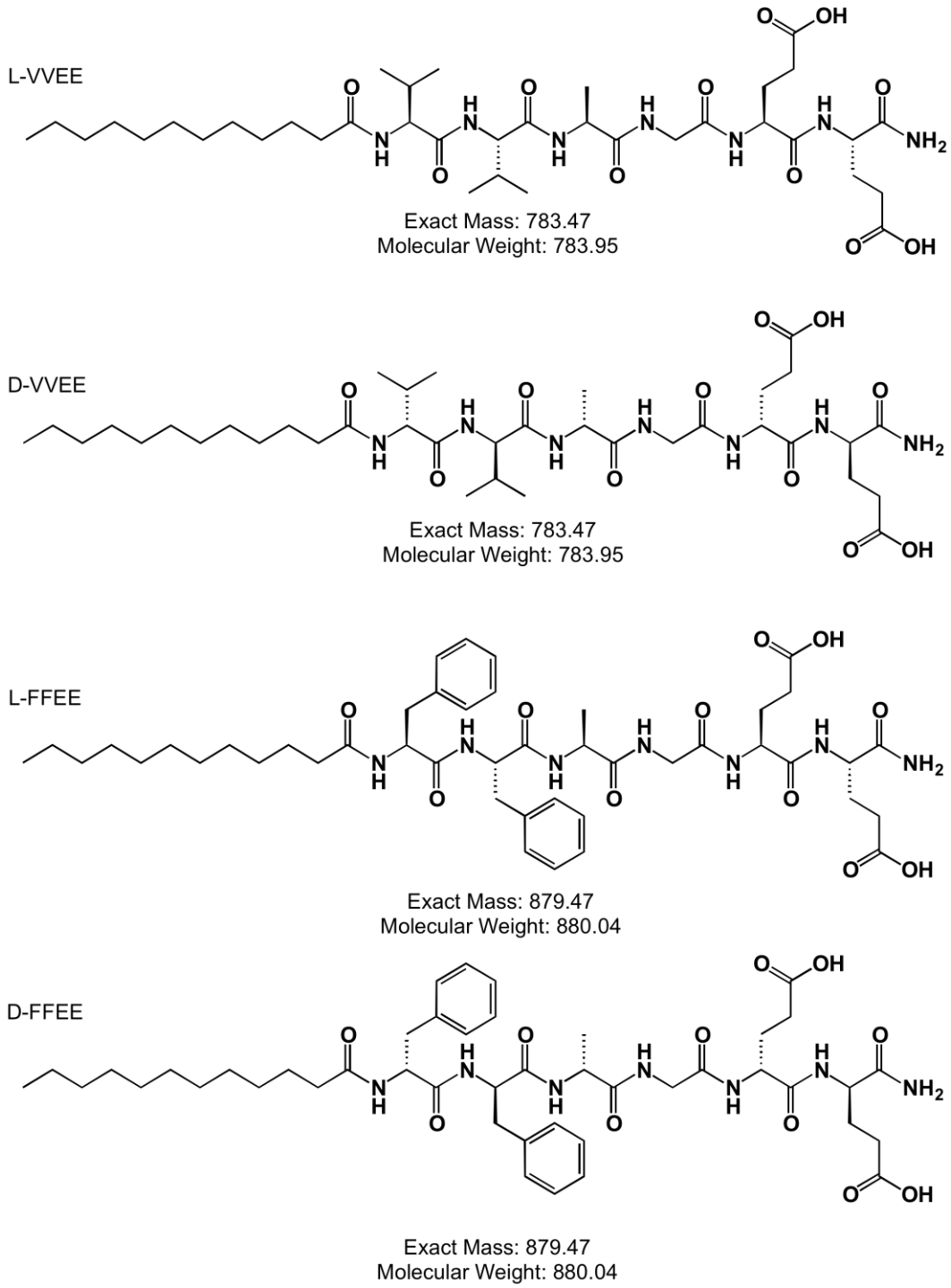

Figure 2.3L-LAURYL-VVAGEE (L-VVEE) , D-LAURYL-vvaGee (D-VVEE) , L-LAURYL-FFAGEE (L-FFE), D-LAURYL-ffaGee (D-FFEE)

L-VVHH

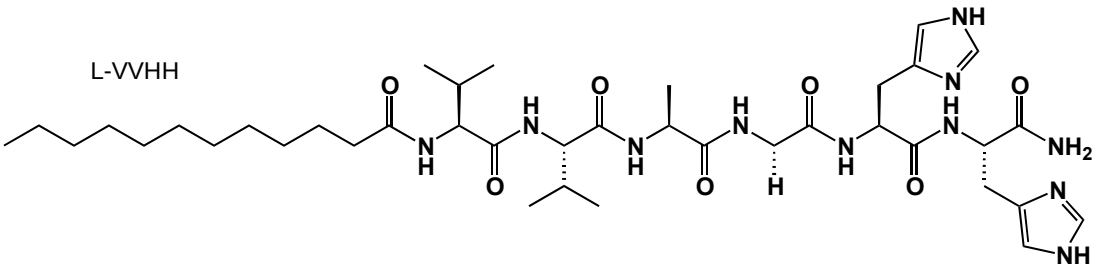

D-VVHH

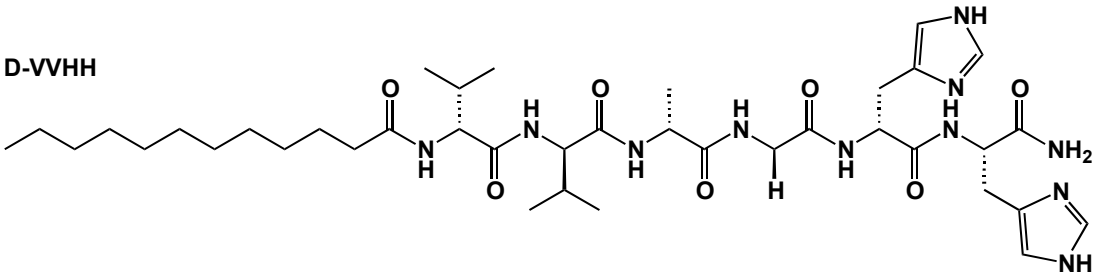

L-FFHH

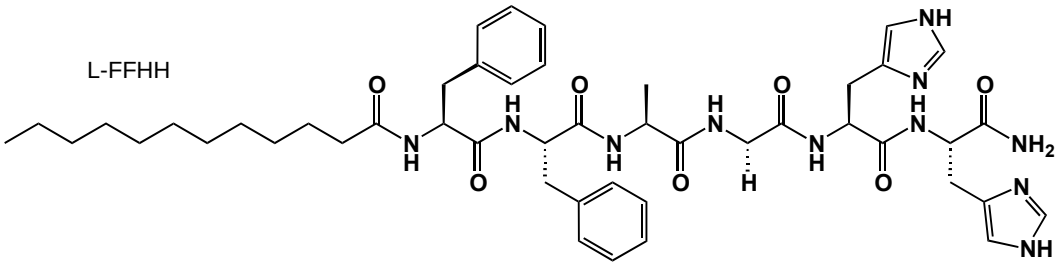

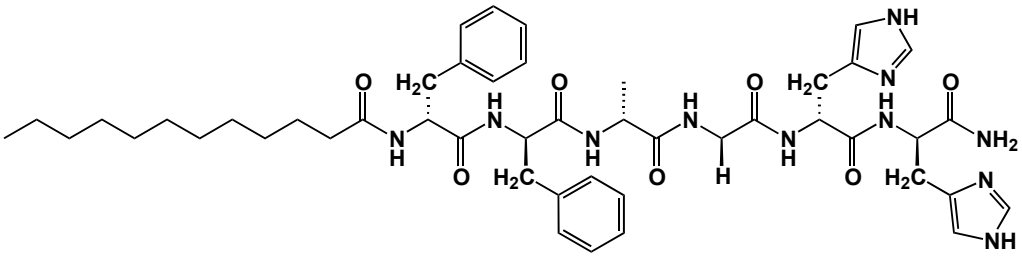

Figure 2.4L-LAURYL-VVAGHH (L-VVHH) , D-LAURYL-vvaGhh (D-VVHH) , L-LAURYL-FFAGHH (L-FFHH), D-LAURYL-ffaGhh (D-FFHH)

After peptide sequences were synthesizedby solid phase peptide synthesis protocol that was explained in the experimental part, all peptides were purified with preparative high-pressure liquid chromatography. All positive peptides were treated with HClsolution and then characterized by Liquid Chromatography and Mass Spectrum (LC-MS). LC-MS results indicate that all peptides were synthesizedwith95% percent purity, whichis just perfect for both in vitro and in vivo experiments. Liquid chromatography and mass results are shown in following pages for each peptide amphiphile molecules. Masses were calculated according to table

Table 2.2. List of molecular weight and exact mass of all peptides

Name	***Sequence***	***Exact Mass***	***Molecular Weight***
L-VVKK	**Lauryl-VVAGKK**	**781.58**	**782.07**
D-VVKK	**Lauryl-vvaGkk**	**781.58**	**782.07**
L-FFKK	**Lauryl-FFAGKK**	**887.58**	**878.15**
D-FFKK	**Lauryl-ffaGkk**	**887.58**	**783.95**
L-VVEE	**Lauryl-VVAGEE-Am**	**783.47**	**783.95**
D-VVEE	**Lauryl-vvaGee-Am**	**783.47**	**783.95**
L-FFEE	**Lauryl-FFAGEE-Am**	**879.47**	**880.04**
D-FFEE	**Lauryl-ffaGee-Am**	**879.47**	**880.04**
L-VVHH	**Lauryl-VVAGHH**	**779.51**	**800.00**
D-VVHH	**Lauryl-vvaGhh**	**779.51**	**800.00**
L-FFHH	**Lauryl-VVAGHH**	**895.51**	**896.09**
D-FFHH	**Lauryl-ffaGhh**	**895.51**	**896.09**

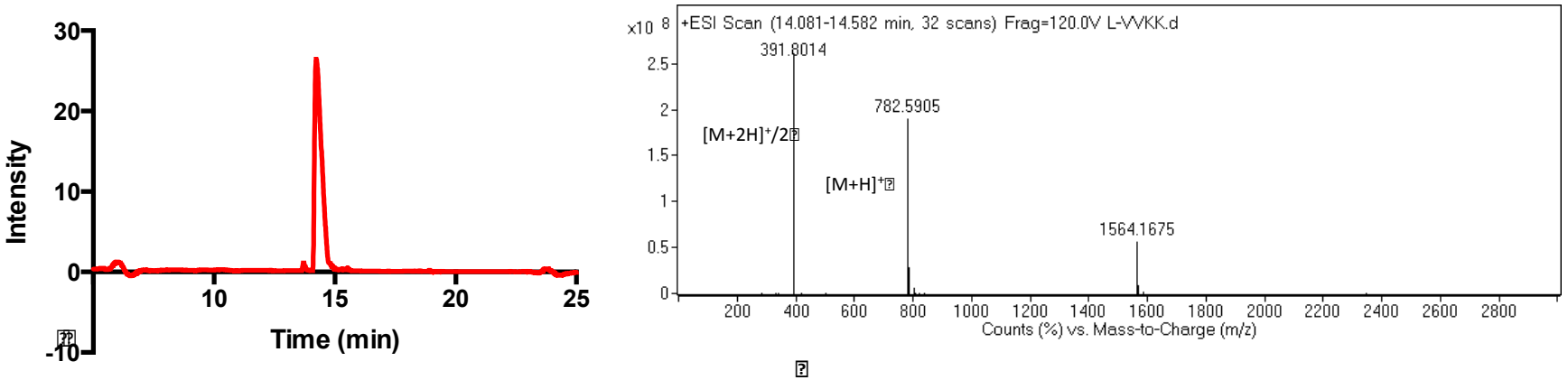

***L*-VVKK:** [M+H]$^+$ (calculated): 782.58, [M+H]$^+$ (observed): 782.5905, [M+2H]$^+$/2 (calculated): 391,79, [M+2H]$^+$/2 (observed): 391.8014

Figure 2.5. Liquid chromatography and mass spectrum of the Lauryl-VVAGKK-Am peptide amphiphile

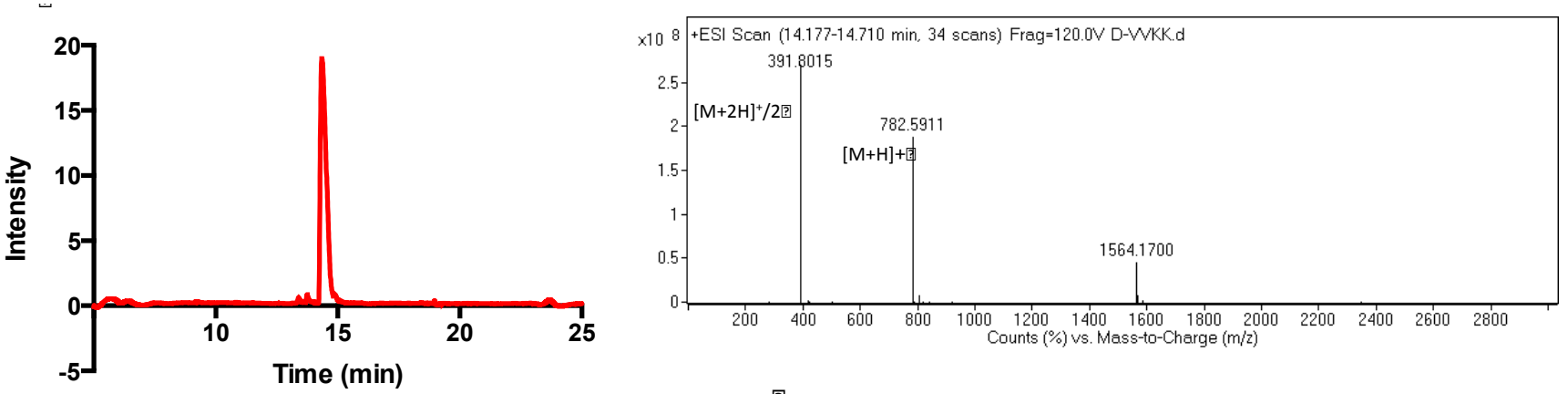

D-VVKK: [M+H]$^+$ (calculated): 782.58, [M+H]$^+$ (observed): 782.5911, [M+2H]$^+$/2 (calculated): 391,79, [M+2H]$^+$/2 (observed): 391.8015

Figure 2.6. Liquid chromatography and mass spectrum of the Lauryl-vvaGkk-Am peptide amphiphile

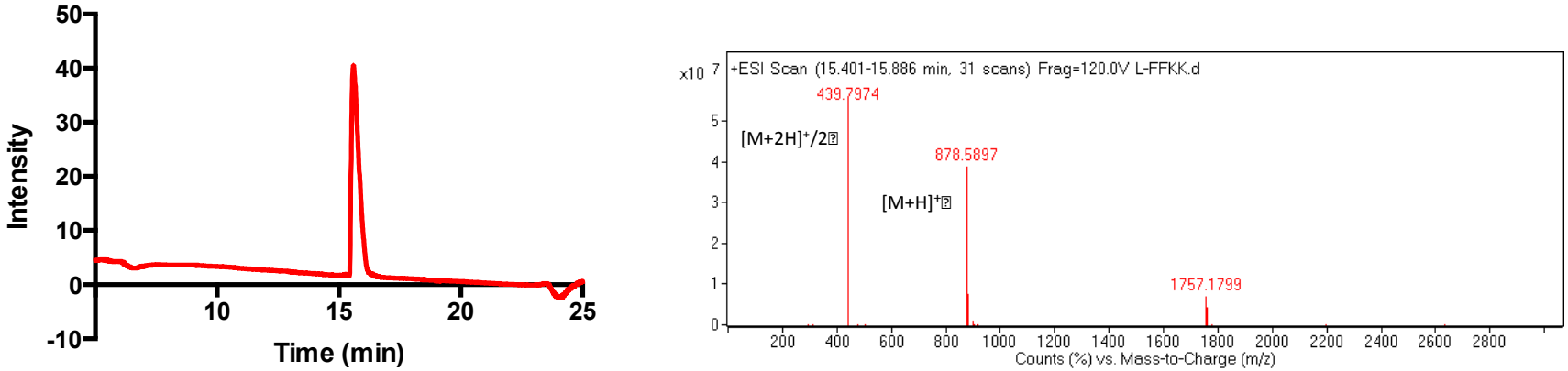

L-FFKK: [M+H]$^+$ (calculated): 878.58, [M+H]$^+$ (observed): 878.5897, [M+2H]$^+$/2 (calculated): 439.79, [M+2H]$^+$/2 (observed): 439.7974

Figure 2.7. Liquid chromatography and mass spectrum of the Lauryl-FFAGKK-Am peptide amphiphile

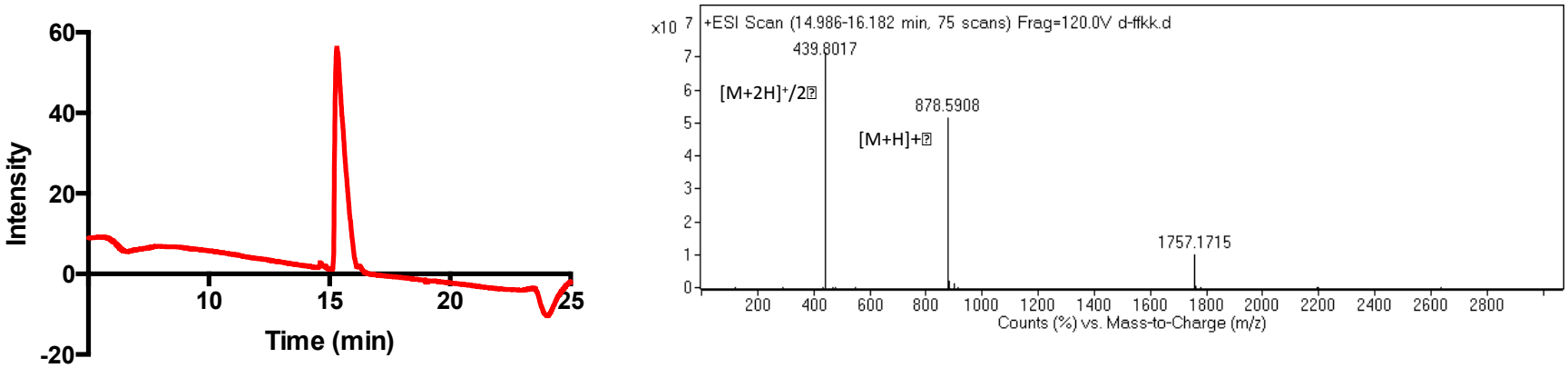

D-FFKK: [M+H]+ (calculated): 878.58, [M+H]+ (observed): 878.5908, [M+2H]+/2 (calculated): 439.79, [M+2H]+/2 (observed): 439.8017

Figure 2.8. Liquid chromatography and mass spectrum of the Lauryl-ffaGkk-Am peptide amphiphile

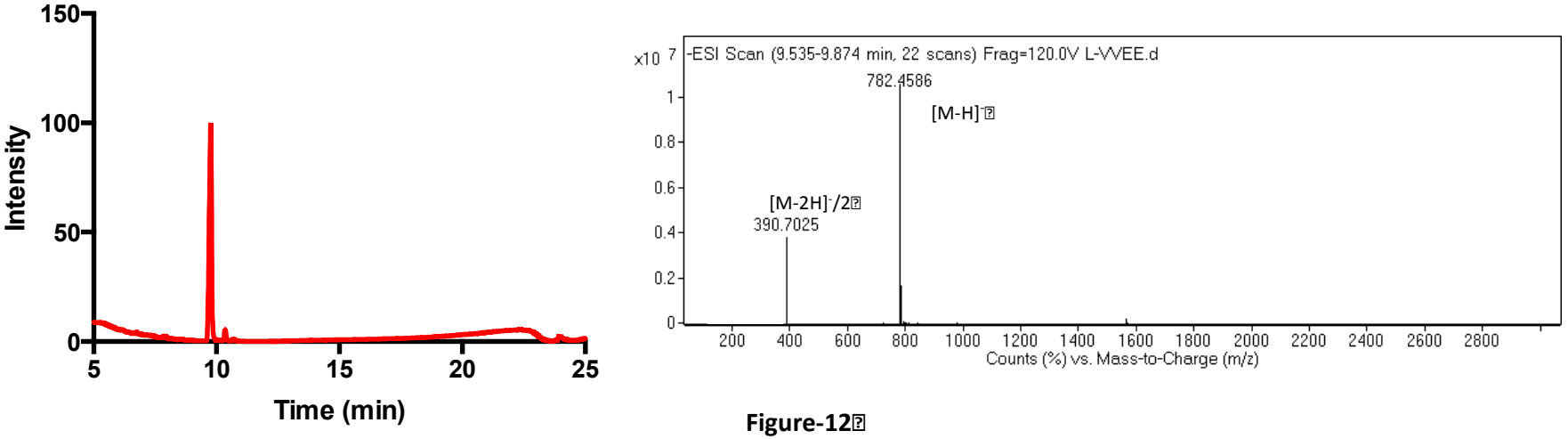

Figure-12

L-VVEE: [M-H]$^-$ (calculated): 782.47, [M-H]$^-$ (observed): 782.4586, [M-2H]$^-$/2 (calculated): 390.735, [M-2H]$^-$/2 (observed): 390.7025

Figure 2.9. Liquid chromatography and mass spectrum of the Lauryl-VVAGEE-Am peptide amphiphile

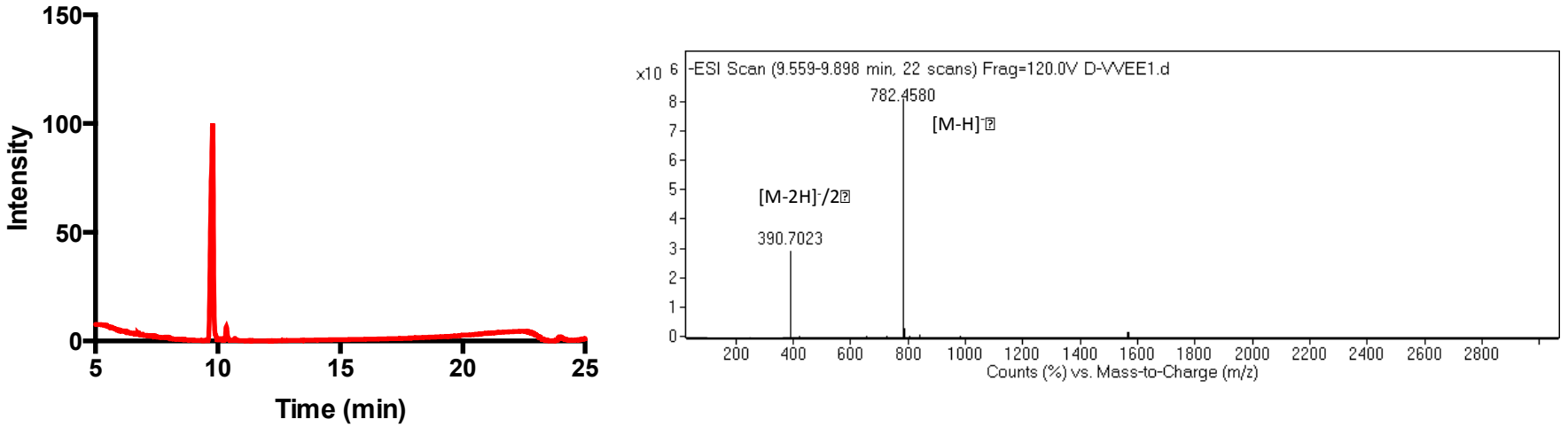

D-VVEE: [M-H]$^-$ (calculated): 782.47, [M-H]$^-$ (observed): 782.4580, [M-2H]$^-$/2 (calculated): 390.735, [M-2H]$^-$/2 (observed): 390.7023

Figure 2.10. Liquid chromatography and mass spectrum of the Lauryl-vvaGee-Am peptide amphiphile

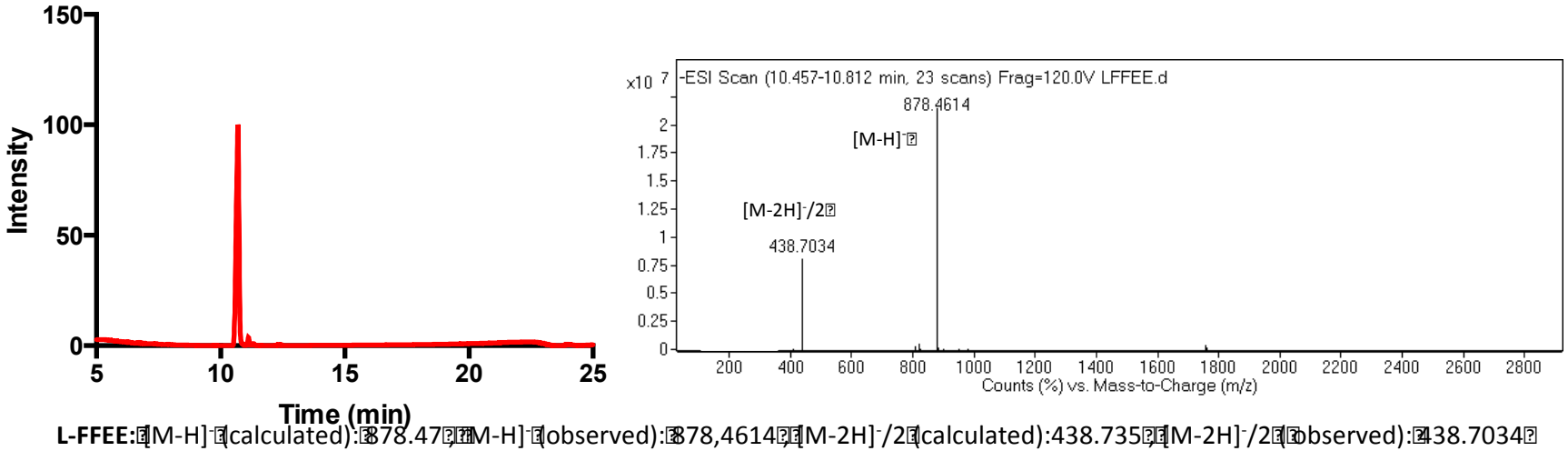

Figure 2.11. Liquid chromatography and mass spectrum of the Lauryl-FFAGeEE-Am peptide amphiphile

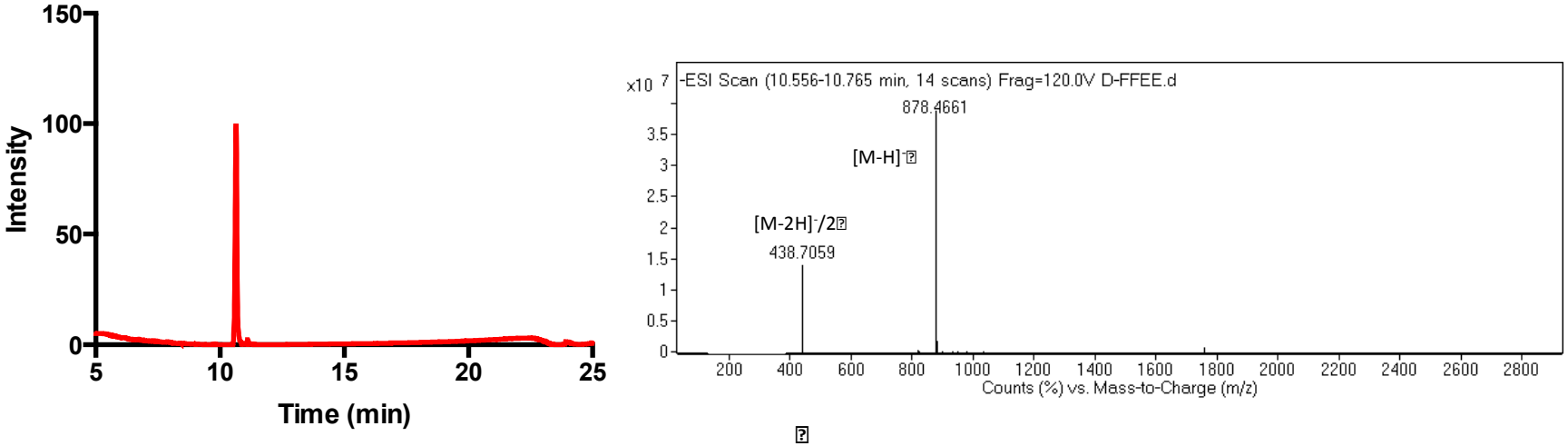

D-FFEE: [M-H]⁻ (calculated): 878.47; [M-H]⁻ (observed): 878,4661; [M-2H]⁻/2 (calculated): 438.735; [M-2H]⁻/2 (observed): 438.7050

Figure 2.12. Liquid chromatography and mass spectrum of the Lauryl-ffaGee-Am peptide amphiphile

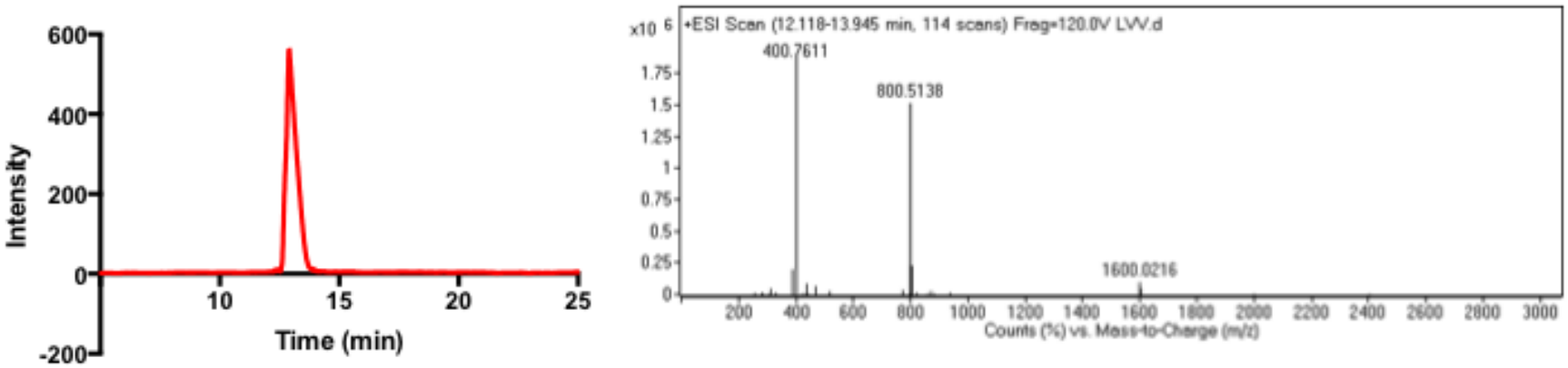

L-VVHH: $[M+H]^+$ (calculated) 800.51, $[M+H]^+$ (observed) 800.5138, [M+2H]/2 (calculated) 400.755, [M+2H]/2 (observed) 400.7611

Figure 2.13. Liquid chromatography and mass spectrum of the Lauryl-VVAGHH-Am peptide amphiphile

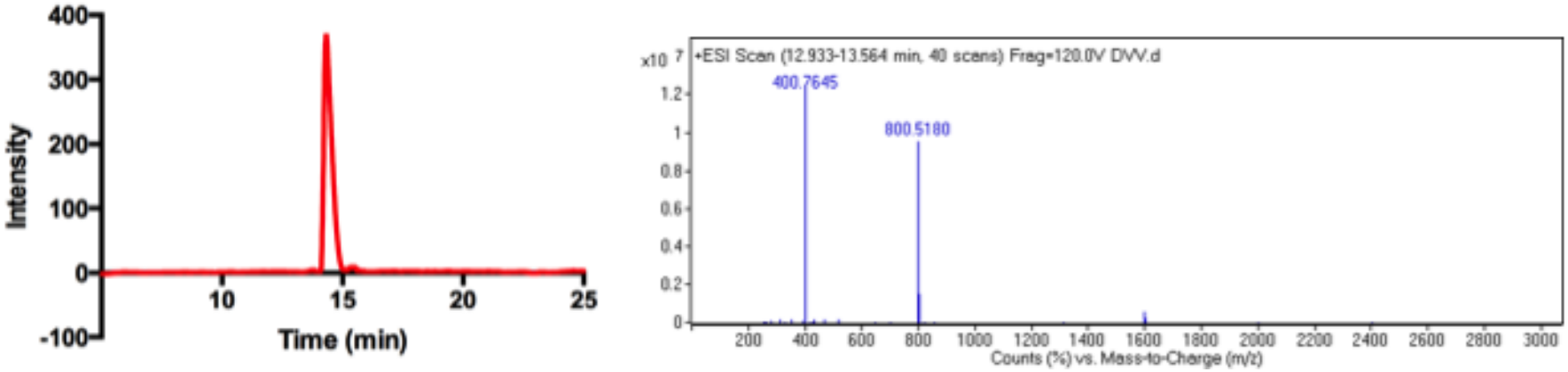

D-VVHH: $[M+H]^+$ (calculated) 800.51, $[M+H]^+$ (observed) 800.5180, [M+2H]/2 (calculated) 400.755, [M+2H]/2 (observed) 400.7645

Figure 2.14. Liquid chromatography and mass spectrum of the Lauryl-vvaGhh-Am peptide amphiphile

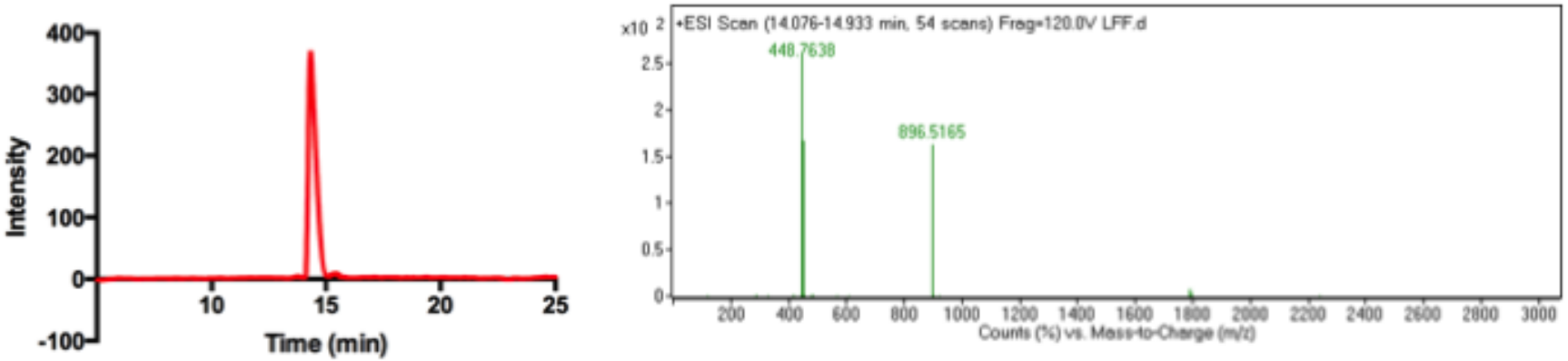

L-FFHH: $[M+H]^+$ (calculated) 896.51, $[M+H]^+$ (observed) 896.5165, [M+2H]/2 (calculated) 448.755, [M+2H]/2 (observed) 448.7638

Figure 2.15. Liquid chromatography and mass spectrum of the Lauryl-FFAGeHH-Am peptide amphiphile

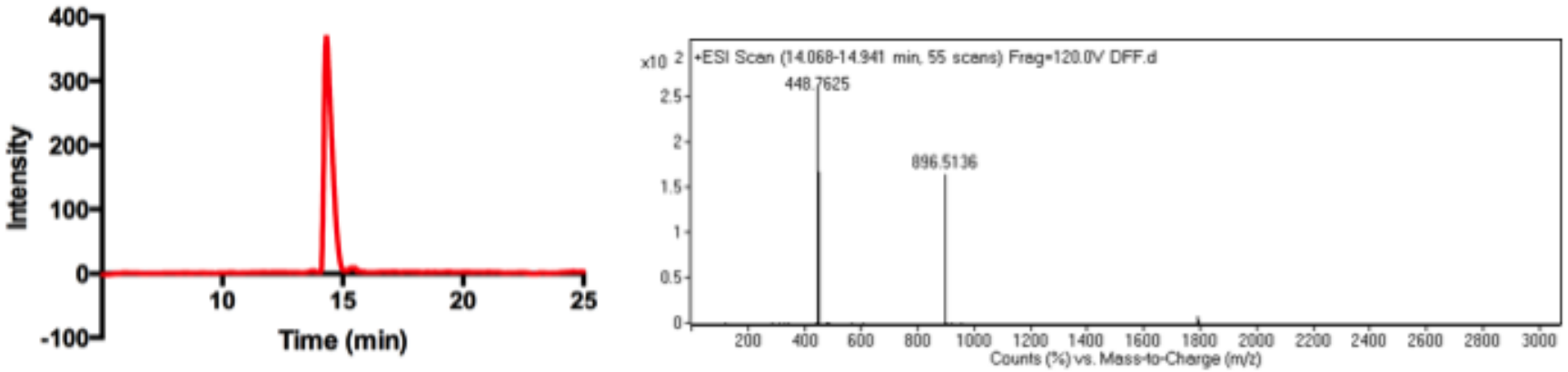

D-FFHH: $[M+H]^+$ (calculated) 896.51, $[M+H]^+$ (observed) 896.5165, [M+2H]/2 (calculated) 448.755, [M+2H]/2 (observed) 448.7638

Figure 2.16. Liquid chromatography and mass spectrum of the Lauryl-ffaGhh-Am peptide amphiphile

After purification of peptide, self-assembly experiments were performed. During the self-assembly of the peptide amphiphile molecules, regulating external and internal factors pretty significant for tuning final supramolecular morphology. In first part of the study, Histidine peptides were used. Histidine peptide has good solubility in water and self-assembly of histidine peptide amphiphile was easily triggered by pH increase. In second part of the study, lysine containing positive peptide amphiphile and glutamic acid peptide amphiphile were used as building blocks of the self-assembly experiments. Lysine also has fine solubility in water. Beside lysine peptide amphiphile quiet useful due to it has ability to form hydrogel both addition of base and charged neutralization with the negative peptide like glutamic acid containing pair of it.

2.3.2 pH-Triggered Chiral Self-Assembly of the Histidine Peptide Amphiphile Building Blocks

Histidine amino acid attracts great attention because it incorporates many interesting feature simultaneously. It is polar amino acid with an aromatic side chain. Thanks to aromatic imidazole side chains of it, in self-assembly systems, histidine peptide amphiphiles can be effected several interactions at the same time. The main interactions that affectassembly of the histidine containing amphiphilic molecules are metal ligand interaction, π-π stacking,hydrophobic[71,72], and hydrophilic interactions. In dynamic self-assembly systems, contribution of all these interactions cause difficulty in controlling morphology of the nanostructures. Therefore in this part of the thesis, we aimed to study self-assembly mechanism of histidine containing peptide amphiphile molecules that have different chirality and β-sheet forming region. For this purpose, first, four different peptide amphiphile (PA) sequences were designed any synthesized. Among these, two PA consist of L-amino acid (L-PA), and other two consist of D-amino acid (D-PA). One of the L-PA and D-PA includes Val-Val sequences in β-sheet forming region and others have Phe-Phe amino acid pair instead of Val-Val sequences. All designed PAs are listed in the Table-2.3.

In order to obtain fine-tuning in the morphology of the self-assembly of the histidine containing peptide amphiphile nanostructures, pH of the systems were adjusted to pKa value of imidazole. Imidazole has a pKa of approximately 6. Below this pH, side chains of the histidines are protonated . Above the physiological pH 90% of the imidazoles are able to form hydrogen bond. In basic condition it behaves like both hydrogen donor and acceptor.[39] Therefore, self-assembly conditions were designed at slightly acidic pH (pH 4.5), near to pKa value (pH 6.5), physiological pH, (pH 7.4) and basic condition (pH 10). The effects of pH differences on morphology and dynamic nature of peptide nanostructures were analyzed with different characterization techniques. For morphological characterization, transmition electron

microscopy (TEM) was used. Chiral behaviors of the PA molecules were monitored with Circular Dichroism (CD). Besides to individual characterization of L-PA and D-PA, self-assembly mechanisms of chiral mixtures of same peptide amphiphile molecules were also characterized with similar techniques. With these experiments, the effects of chiral mixtures to the nature of self-assembly of dynamic chiral peptide amphiphile molecules were examined. In addition to chirality of peptides, differences in the β-sheet forming region of peptide amphiphiles also lead to obtain self-assembled nanostructures with different morphologies at same conditions**.**

Table 2.3. Histidine peptide amphiphile building blocks used in pH-triggeredchiral self-assembly

HH
L-Lauryl-VVAGHH (L-VVHH)
L-Lauryl-FFAGEE (L-FFHH)
HH
D-Lauryl-VVAGEE (D-VVHH)
D-Lauryl-FFAGEE (D-FFHH)

Several chiral self assembly trials were performed with morphologic and spectroscopic characterization of nano structures. Secondary structures of chiral peptides amphiphiles were characterized with Circular Dichroism (CD). As stated previously, typical perfect β-sheet secondary structure can be identified from maximum peak at 195 nm and a minimum peak at 216 nm wavelength in the spectra. Circular Dichroism results of VVHH and FFHH peptides at pH 4.5, pH 6.5, pH 7.4 and pH 10 shown in figure-2.17 and figure-2.18. In all CD results it was obtained characteristic β-sheet signal. However the red shift in the spectrums indicates slight distortion from perfect β-sheet secondary structure due to the twisted β-sheet

formation. [73] The red shiftarises from decrease in the hydrogen bond energy due to twisting β-sheet forming. Because of π-π interaction between the Histidine moieties, building blocks were not assembled with a certain 90^0 degree. So they form twisting β-sheet secondary structure with a larger hydrogen bond angle, longer bond length and lower bond energy Therefore characteristic signal of β-sheet is obtained in higher wavelength. Moreover, at pH 10 it was obtained extra peaks around 225 nm and 240 nm (Figure-2.17-d). These extra peaks come from orientation change in the imidazole groups because of high propensity to form hydrogen bonding in their basic form [74]. Moreover, in CD signal of the L-VVHH and D-VVHH mirror symmetry was achieved. This means that, these molecules have similar secondary structures with the reverse chirality.

As for L-FFHH and D-FFHH peptide amphiphile nanostructures, again, similar red shifted twisted β-sheet signals were obtained at different pH values. Different than pH 4.5 and 6.5, it was obtained extra positive peak at 225 nm and 240 nm at pH 7.4 and 10. (Figure-2.18-c,d). These peaks arose from contribution of both phenyl alanine and histidine aromatic moiety to the supramolecular organization of peptide amphiphile molecules. Again almost symmetric signals acquired for reverse chiral molecules

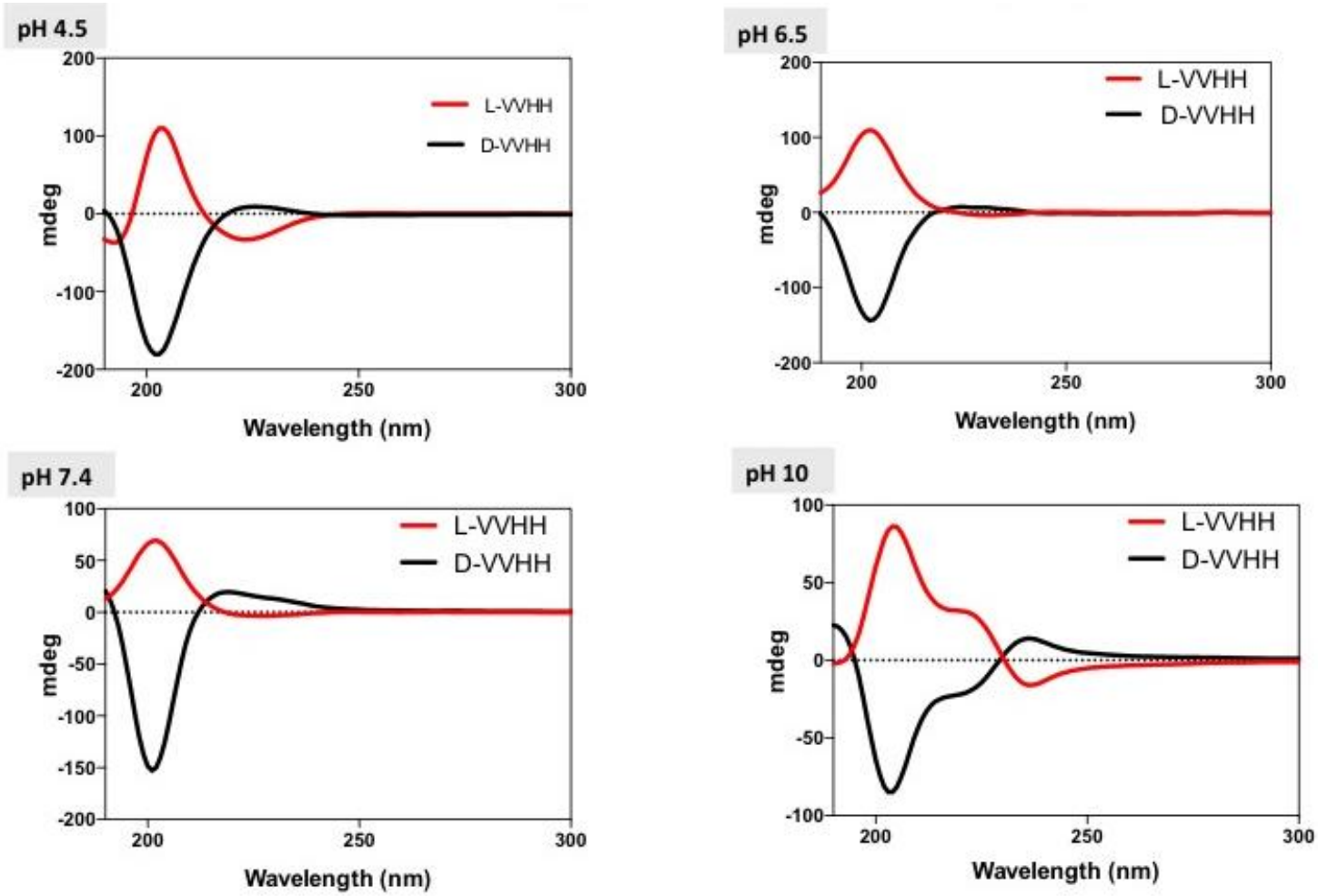

Figure 2.17L-VVHH and D-VVHH PA at pH 4.5, pH 6.5, pH 7.4 pH 10

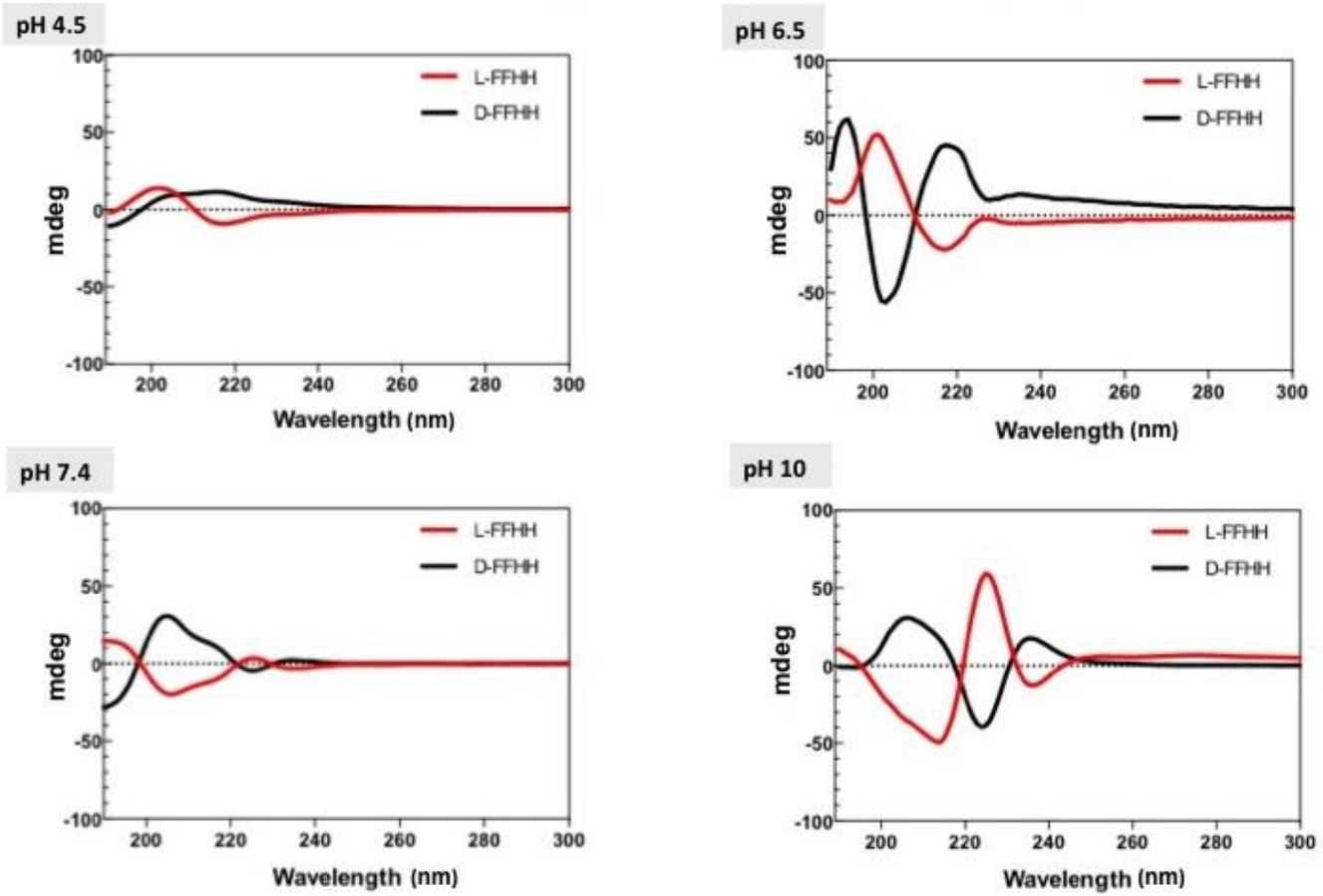

Figure 2.18 L-FFHH and D-FFHH PA at pH 4.5, pH 6.5,pH 7.4 pH 10

Structural characterization of PA nanostructures was achieved by TEM imaging technique. (Figure-2.19,20,21,22) In acidic pH all of the four peptides have a tendency to form nanosheet structures. At pH 6,5 and pH 7.4, L-VVHH and D-VVHH form twisted nanofibers and twisting ribbon with respectively. Upon increase of the pH, imidazole groups are deprotonated but around isoelectric point, which is pH 6.5, still keeps positive charge. Change in the charge of the imidazole group, effects to Coulombic interaction between the building blocks and packing of the molecules. Above isoelectric points, imidazole groups get neutralized and π-π interaction dominates de supramolecular organization. Therefore, at pH 10, L-VVHH and D-VVHH PA molecules generate peptide nanotubes due to the multilayer molecular packing of the building block. This packing first produce large sheet like structures, these sheets curling due to π-π stacking between the aromatic groups and form helical ribbons. Simultaneously, molecules on the edges of the ribbon, grows to close the pitches of helices by hydrogen bonding and form a nanotube. While fibers areapproximately 8 nm in diameter, nanotubes have a diameter around 110 nm. Similar molecular packing behavior was observed for L-FFHH and D-FFHH peptide nano structures as well. While L-FFHH and D-FFHH PA molecules for nanosheet at acidic pH, around isoelectric point, they form twisted nanofibers. However, in basic condition, L-FFHH and D-FFHH produce short twisting ribbons and they cannot form nanotube like L-VVHH and D-VVHH PA molecules. Because these PAs consist of phenyl alanine and histidine aromatic group at the same time, there is two competitive π-π stacking interaction includes to organization of molecules. This lack of elasticity of the molecules cannot allow the nanostructures expanded and closed as nanotube.

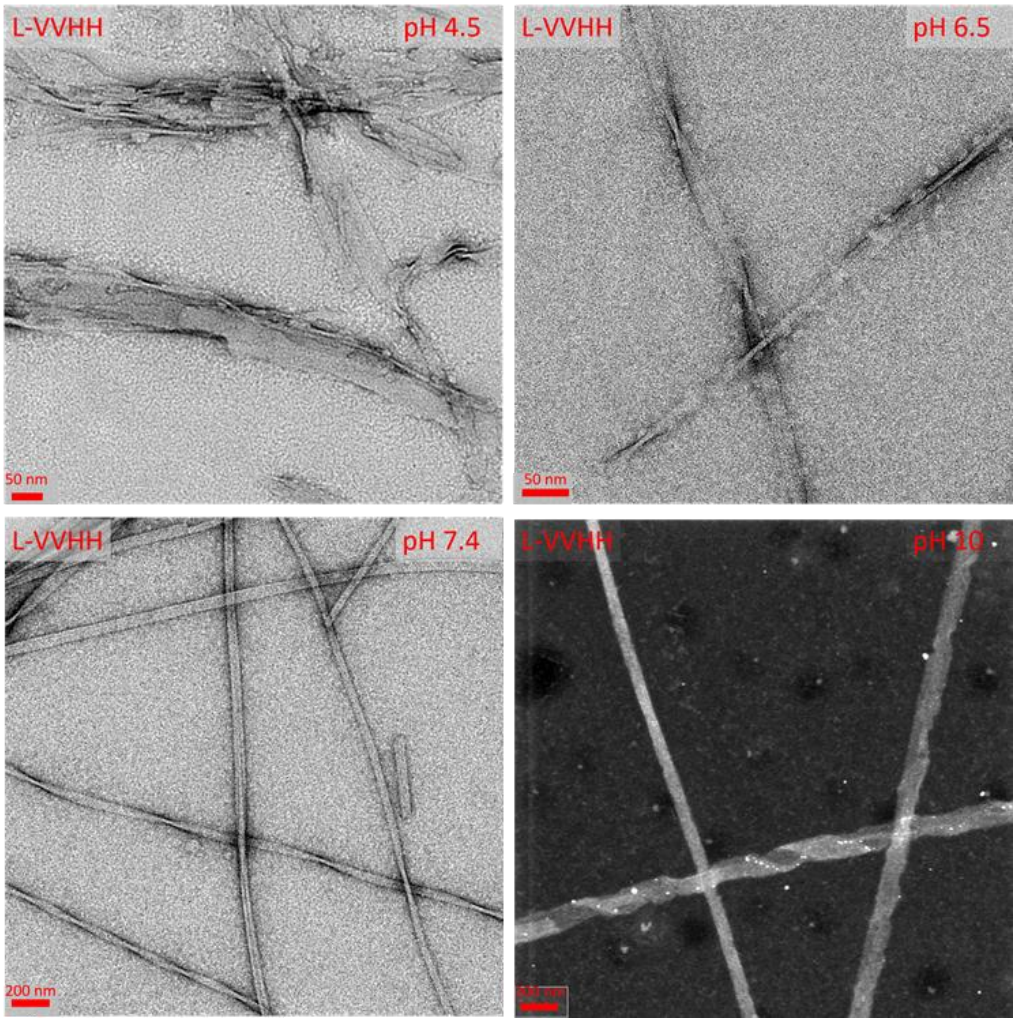

Figure 2.19TEM images of L-VVHH at different pH

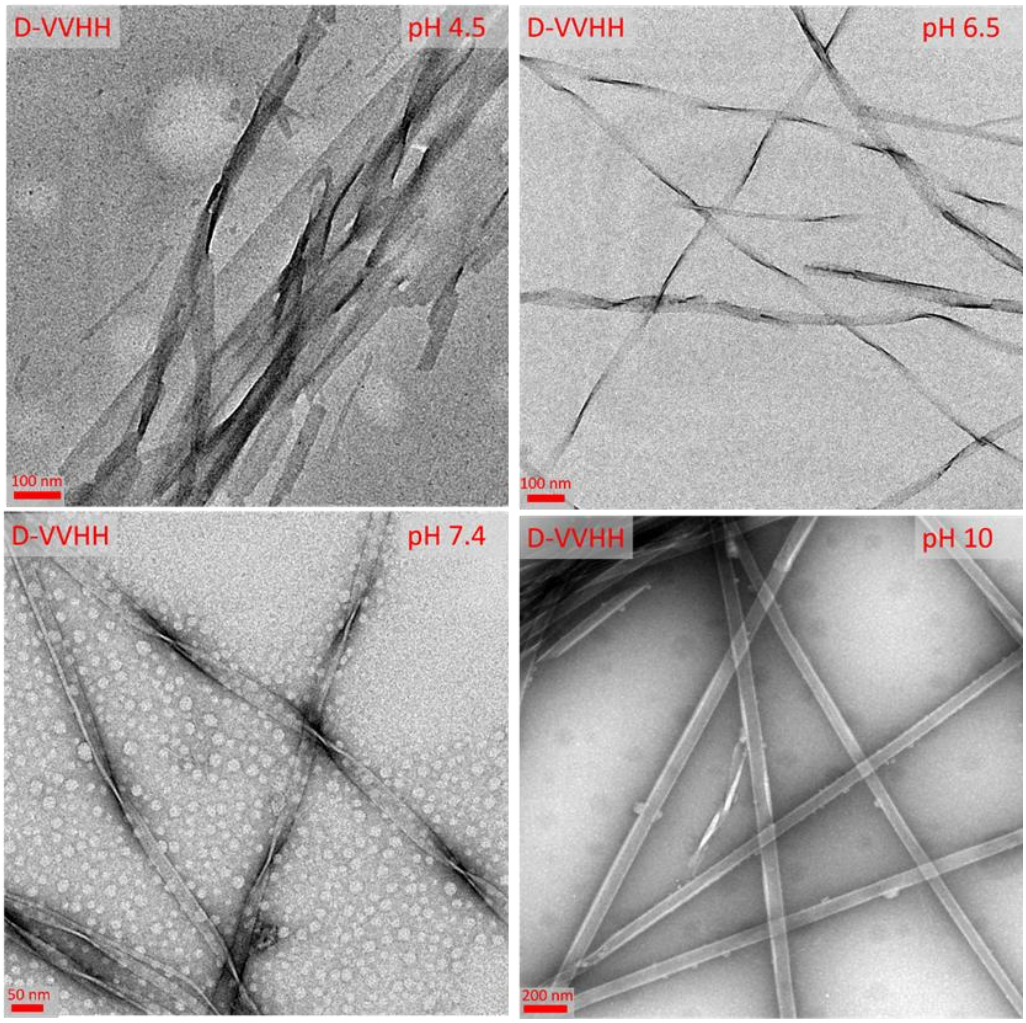

Figure 2.20TEM images of D-VVHH at different pH

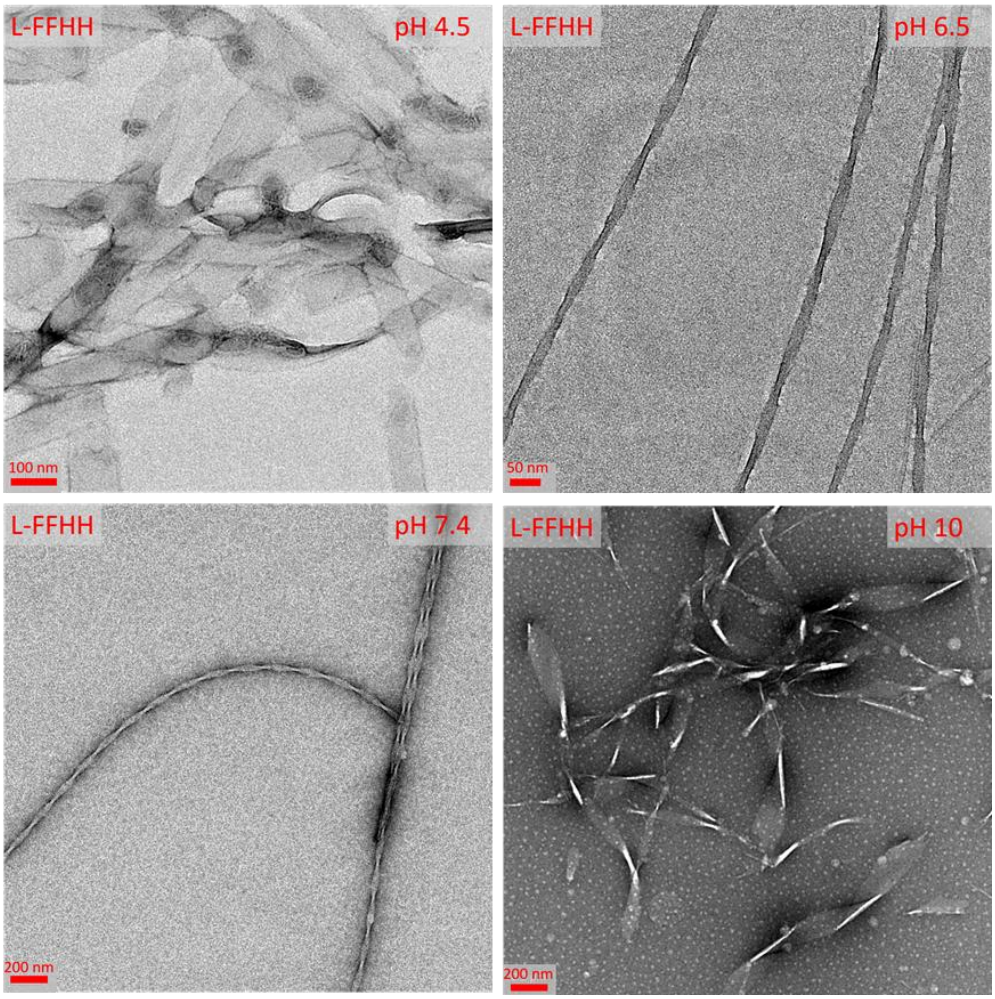

Figure 2.21TEM images of L-FFHH at different pH

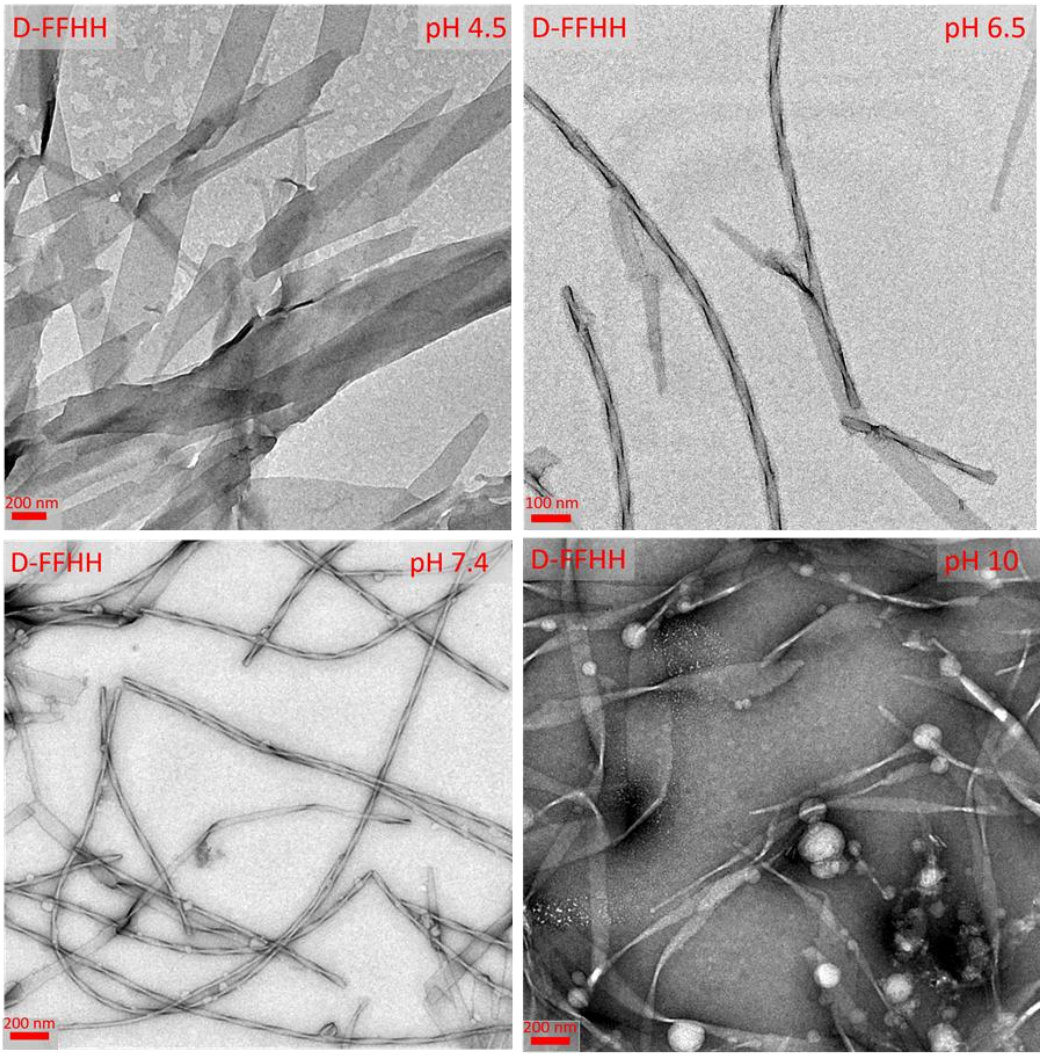

Figure 2.22TEM images of D-FFHH at different pH

Then, chiral mixtures of valine containing histidine peptide amphiphile was studied. Peptides were mixed, according to sample preparation protocol in HFIP, which explain in experimental part. As stated previously, L-PA and D-PA were mixed different molar ratio that shown in **Figure 2.23.** Upon increases of D-PA

amount in the L-PA solution, β-sheet signal decrease, and become zero in 50% racemic mixture. When D-PA amount to exceed the L-PA amount β-sheet signal turns to mirror symmetry and it resembles to D-PA. Remarkably, when morphological change was characterized by TEM it was found out that, L-PA and D-PA form nanotube but interestingly racemic mixtures produce nanofibers. (Figure 2.23**)**

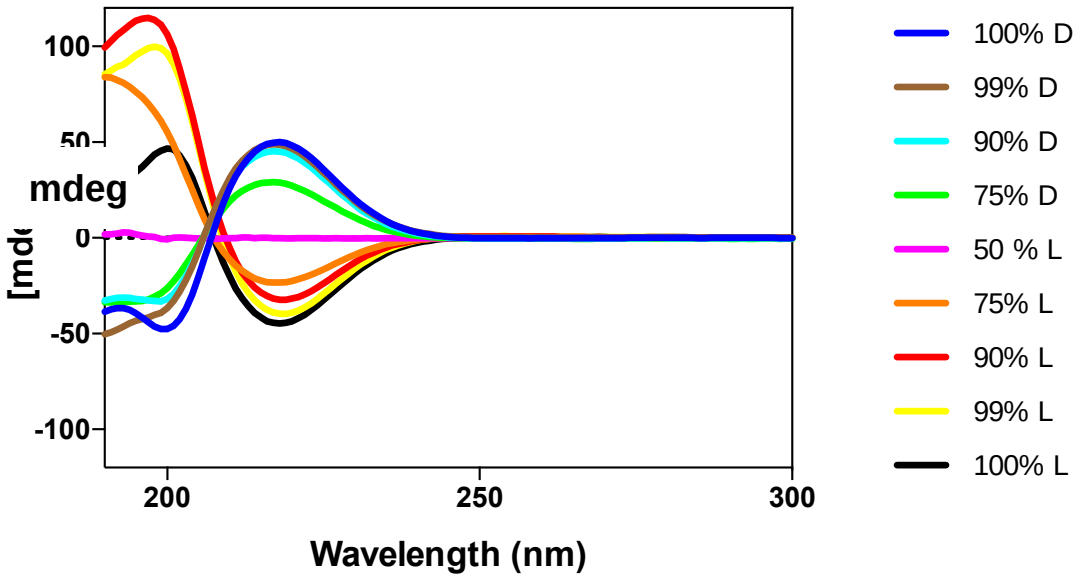

Figure 2.23 Chiral Mixture of L-VVHH and D-VVHH PA with different molar ratio

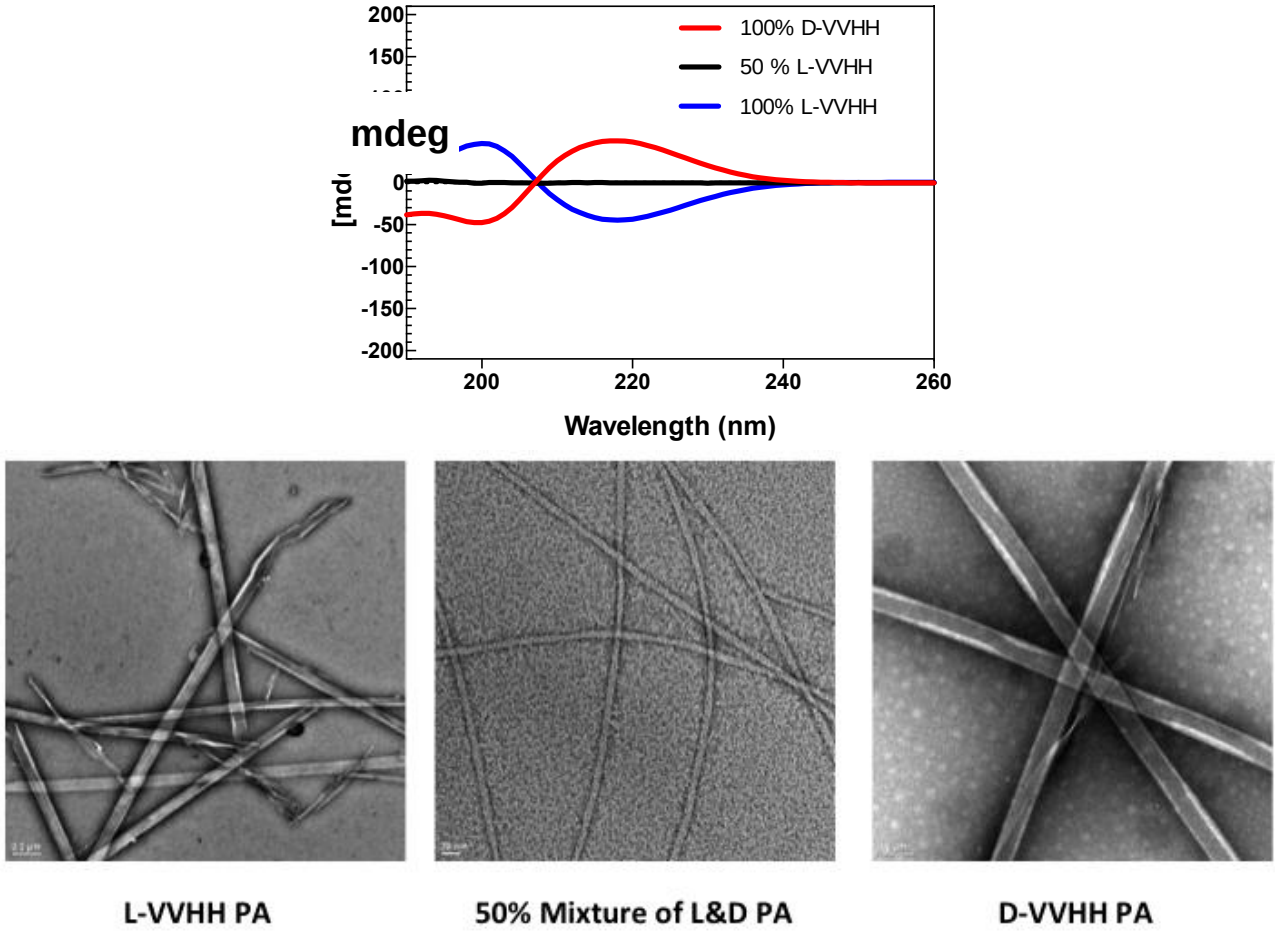

Figure 2.24 Circular Dichroism results and TEM imafge of L-VVHH & D-VVHH racemic mixture

2.3.3 Self Assembly of the EE/KK Peptide Amphiphile Upon Charged Neutralization.

In next part of thesis, self-assembly mechanism of valine and phenylalanine containing positive and negative peptide amphiphile investigated both for L and D form of them. For positive two charges, lysine-lysine moiety, for negative two charges glutamic acid-glutamic acid residue included to sequences. List of all designed peptide provided in Table-2.4

L- PAs	**KK**	**EE**
VV	Lauryl-VVAGKK (L-VVKK)	Lauryl-VVAGEE (L-VVEE)
FF	Lauryl-FFAGKK (L-FFKK)	Lauryl-FFAGEE (L-FFEE)
D-PAs	KK	EE
VV	Lauryl-vvaGkk(D-VVKK)	Lauryl-vvaGee (D-VVEE)
FF	Lauryl-ffaGee (D-FFKK)	Lauryl-ffaGee (D-FFEE)

Table 2.4. pH Trigger and charged neutralize chiral self-assembly of the EE/KK peptide amphiphile building blocks

After all peptides were synthesis and purified, hydrogen-bonding pattern in the self-assembly hydrogel systems was characterize by Circular Dichroism. β-sheet secondary structures of peptides were detected with Circular Dichroism (CD). As stated previously in 1.4c, typical β-sheet secondary structure can be identified from maximum peak at 195 nm and a minimum peak at 216 nm wavelength in the spectra.

According to Circular Dichroism results which was shown in Figure: 2.25, L-VVKK PA, D-VVKK, L-FFKK PA and D-FFKK PA give characteristic β-sheet

signal in the spectrum at pH 10. At this pH enlargement of the peak around 220 nm wavelength in the spectra of L-FFKK PA and D-FFKK PA, comes from phenyl alanine contribution to the supra molecular organization. Same β-sheet hydrogen bonding trend was observed in L-VVKK/ L-VVEE PA mixture and D-VVKK / D-VVEE PA mixture as well at pH 7 that L-FFKK/ L-FFEE PA mixture and D-FFKK / D-FFEE PA mixture form β-sheet secondary structure at neutral pH. Moreover the peak around 220 nm wavelength indicates to supra molecular chirality contribution to the spectra.

For understanding morphology of peptide amphiphiles, nanostructures were imaged by STEM and TEM. L-VVKK and D-VVKK form nanofiber both pH 10 and pH 7 (Figure2.26a,b,e,f) In the case of phenyl alanine containing peptides, twisted nanofibers were detected. (Figure-2.26 c,d,g,h). Due to the π-π stacking between two phenylalanine side chain, generate the twisting structure in stead of straight nanofiber like in valine containing sequences. TEM image of L-FFKK/EE twisted nanofiber with 17.90 nm average diameter size and 52.79 nm average pitch size and STEM image of D-FFKK/EE twisted nanofiber with 15.33 nm average diameter size and 45.92 nm average pitch size.

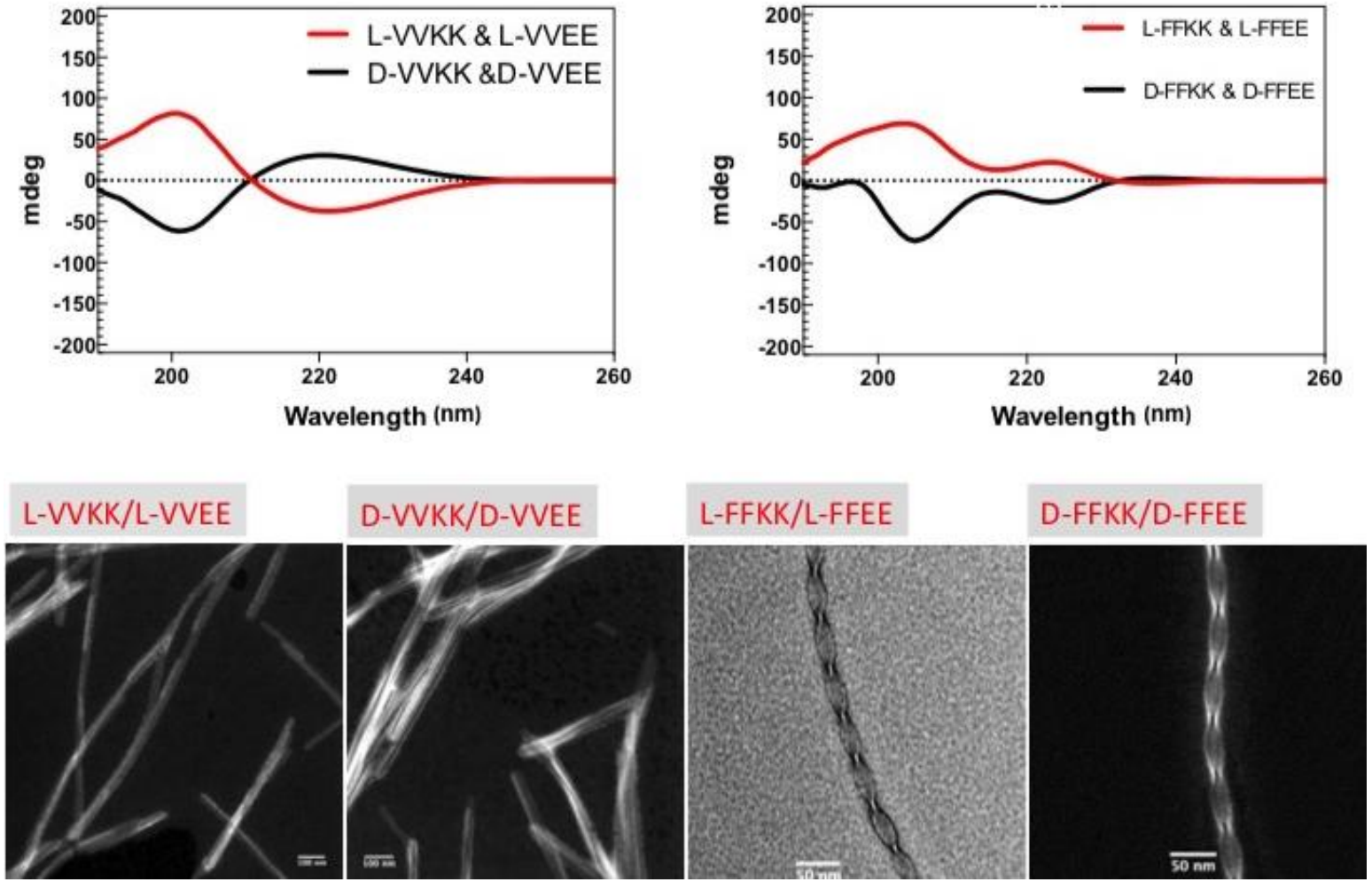

Figure 2.25CD and TEM analysis of L-VVKK/L-VVEE, D-VVKK/D-VVEE, L-FFKK/L-FFEE, D-FFKK/D-FFEE PAs at pH 7

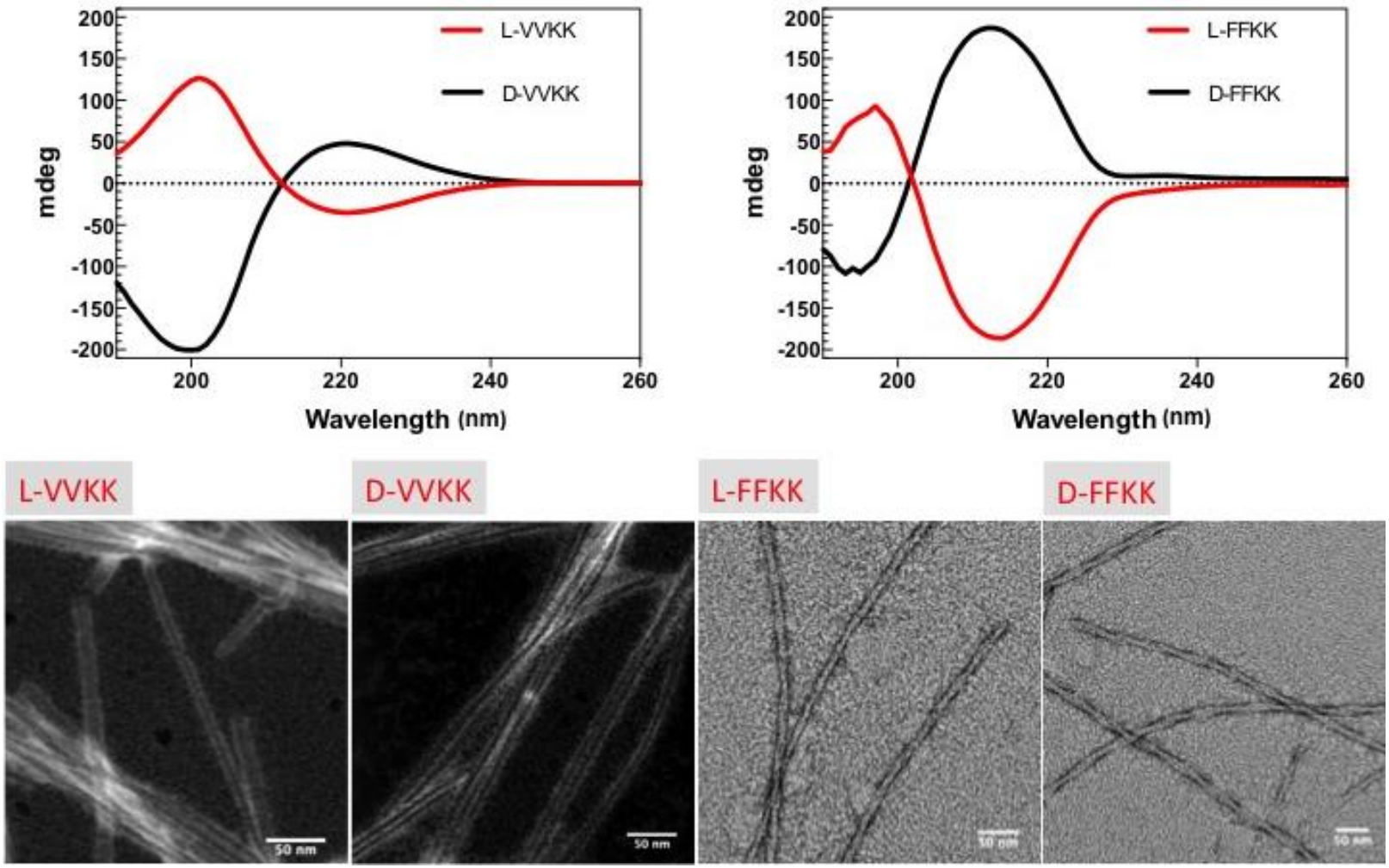

Figure 2.26CD and TEM analysis of L-VVKK, D-VVKK , L-FFKK, D-FFKK PAs at pH 10

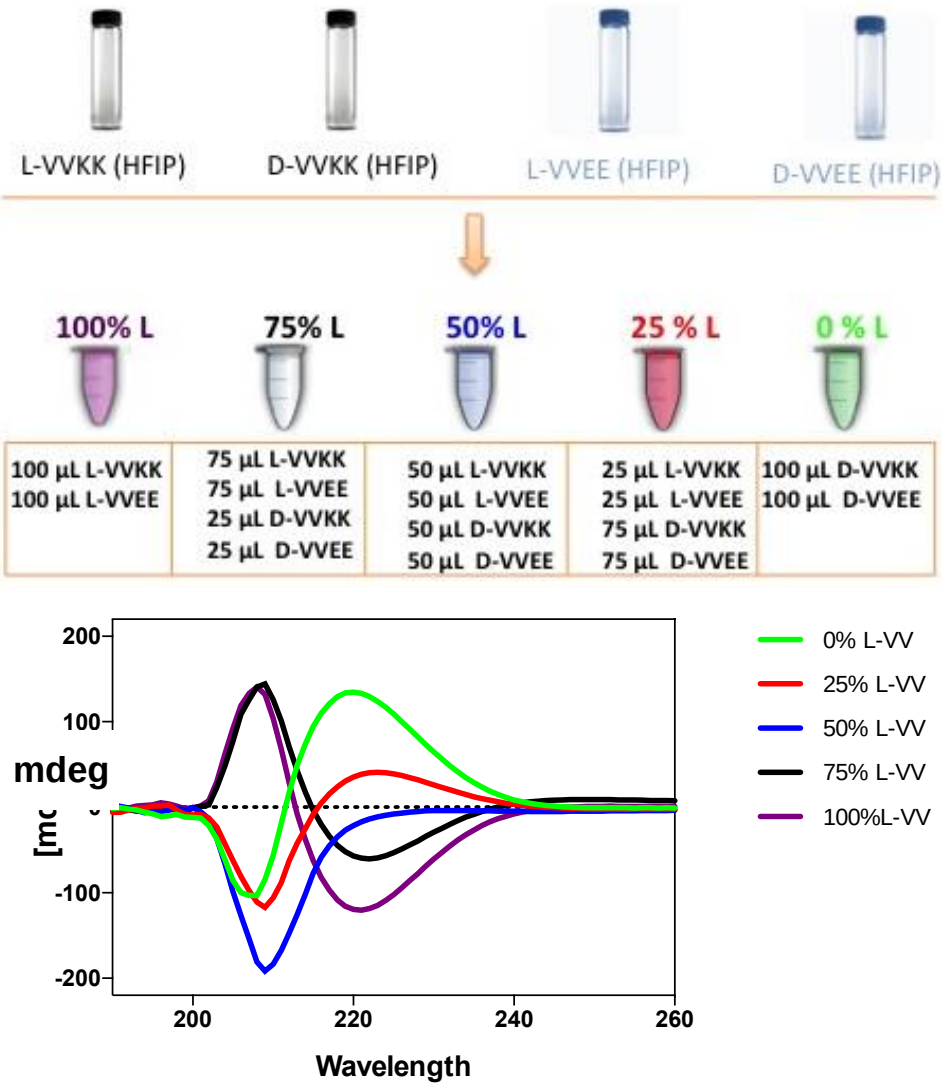

Figure 2.27CD spectrum of chiral mixtures

To prepare chiral mixtures of peptide amphiphile, first peptides which have different chirality are mixed in hexafluoro-2-propanol (HFIP). The PA molecules were found to exist as disassembled monomers in the good Hydrogen bond donor solvent HFIP. Therefore mixtures that has 100% 75% 50% 25% 0% ratio L VS D peptide ratio prepared first in HFIP. Then, all mixture was dissolved in water after they were dried under vacuum and all HFIP removed. Thanks to this procedure, every single peptide in the mixture face with water at the same time, and self-assembly process start simultaneously for each building block. Moreover, mixing peptides in HFIP before assemble them in water, provides, L and D form of peptides assemble together. Circular dichroism results are indicates that (Figure: 2.27) when L and D form mix with 3:1 (75% L) and 1:3 (25%L) L vs D ratio gave almost symmetric β-sheet secondary structure. Interestingly, when L-PA and D- PA mix with 1:1 ratio, there was obtain intense negative peak which dominated by D-PA. Although L-VVKK/EE and D-VVKK/EE form straight nanofiber in pH 7, they were form twisting nanofiber in 75% L and 25% L mixtures. In 75% L twists occur in the direction of left handed, (Figure 3-a) and in 25% L twists were right handed. This means that, addition of D-PA to the L-PA disturb to straight formation of nanofibers and cause twisting during the self assembly. Upon addition of D-PA, twisting amount decrease and minimize in 50% mixture. When L-PA and D-PA were mixed with equal amount, that was obtained, not straight nanofiber but slim turning in the direction of right handed. (Figure 3c) This slight right handed turn strengthen to claim of D-PA dominancy which achieved in CD spectra (Fig.3-d). When D-PA amount is getting higher than L-PA amount in direction of twisting started to change left handed to right handed. Right handed twisted fibers in 25 % L-PA and 75% D-PA mixture can be obtained from TEM (Figure: 2.27)

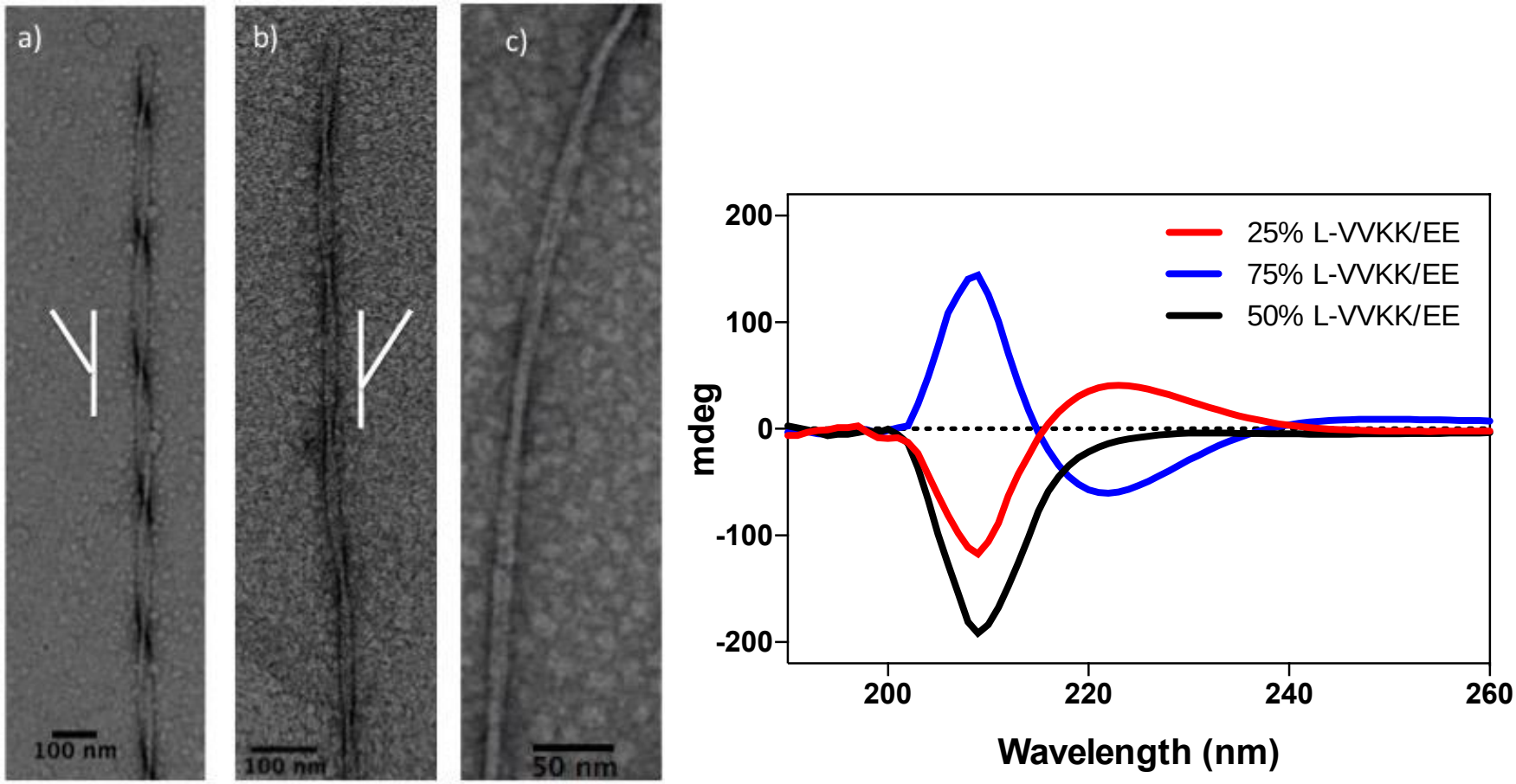

Figure 2.28:L and D form of L-PA and D-PA mixture with 3:1 (75% L) and 1:3 (25%L) L vs D ratio

Chapter 3

3. Conclusions and Perspectives

In this thesis, self-assembly mechanisms of the supramolecular chiral peptide nanostructures were studied. Self-assembly is one of important bottom tool for construction of the high aspect ratio supramolecular structures from different chiral peptide amphiphile building blocks. In this line, fist chiral peptide amphiphile building blocks were designed and synthesized according to solid phase peptide synthesis protocols, which is the most famous and Nobel Prized technique in the chemistry field. After synthesis, their chemical compositions were characterized by using Liquid Chromatography and Mass Spectrum (LC-MS).

Self-assembledsystems have very dynamic nature and similar inter or intra molecular interactions can trigger this process. For example hydrogen bonding, van der Waals interaction, π-π stacking, hydrophobic interactions, electrostatic interactions, metal ion to ligand coordination, solvent effect can effects to self-assembly construction. In this thesis, pH trigger and charge neutralization were preferred as a driving force of the self-assembly process. First, pH trigger self-assembly mechanism of the histidine containing chiral peptide amphiphile nanostructure were characterized at different pHs. According to characterization of secondary structures of L-VVHH –D-VVHH, L-FFHH and D-FFHH, they have characteristic β-sheet signal in circular dichroism. However that signal was obtained red shifted due to the change in the bond angle of peptide amphiphile organization. As for their morphology, below isoelectric point of the histidine group, nano sheet structure was observed for each peptide. Upon to the

increases of pH, it turns to twisted fiber, twisted ribbon. In basic condition helical ribbons were achieved. L-VVHH and D-VVHH PA this large ribbons closed as nanotubes as a results of the π-π interaction between imidazole groups at this basic pH. However, L-FFHH, D-FFHH, L-FFHH and D-FFHH only form twisted short but wide ribbons, because the competitive two π-π stacking aromatic region resulted loose of elasticity of the nanostructures.

In the next part of the study, self-assembly conditions and its effects on the morphology was studied upon charged neutralization of the two oppositely charged peptide amphiphile molecules. For this aim, L-VVKK, D-VVKK, L-FFKK, D-FFKK, L-VVEE, D-VVEE, L-FFEE, D-FFEE peptide are synthesized as building blocks of the self-assembly system. Charged neutralization experiment performed at neutral pH. The pH triggers self-assembly of the L-VVKK, D-VVKK, L-FFKK, D-FFKK at pH accomplished as control of the supramolecular nanostructures the pH neutralization experiment. Spectroscopic characterizations have shown that positive PAs at pH 10, and KK/EE PA mixtures at pH 7 have β-sheet secondary structures. but negative PAs have not. Inverse chiral sequences gave almost symmetric reverse chiral signal in circular dichroism. Differences in PA sequences provide morphological differences; for example valine containing PAs form nanofibers, but phenylalanine containing PAs form twisted nanofibers. Moreover, oppositely charged PA mixtures form more rigid nanostructures in neutral pH. Most interestingly, mixing reverse chiral PAs with different 75% L and 25% D ratio, turning in the fiber nanostructures was obtained.

Here we investigated fine tuning of morphology of the histidine, which controls final structures by the chiral peptide amphiphiles due to pH driven self-assembly. Moreover, similar morphology control was achieved by charged neutralization self-assembly of oppositely charged chiral peptide amphiphile nanostructures. We believe that these well-defined nanosystems canbe used as a functional nanomaterial for various applications.

Bibliography

1. Lichtenthaler, F.W. Emil fischer, his personality, his achievements, and his scientific progeny. Eur. J. Org. Chem. 2002, 24, 4095–4122

2. Fischer, E.; Fourneau, E. Ueber einige derivate des glykocolls. Ber. Dtsch. Chem. Ges. 1901, 34, 2868–2877.

3. *Merrifield R.B. (1963). "Solid Phase Peptide Synthesis. I. The Synthesis of a Tetrapeptide". J. Am. Chem. Soc.* ***85*** *(14): 2149-2154*

4. "The Nobel Prize in Chemistry 1984". Nobelprize.org. Nobel Media AB 2014. Web. 14 Nov 2015

5. Sabatino, G. and A.M. Papini, *Advances in automatic, manual and microwave-assisted solid-phase peptide synthesis.* Current opinion in drug discovery & development, 2008. **11**(6): p. 762-770.

6. Chan, W. and P. White, *Fmoc Solid Phase Peptide Synthesis: A Practical Approach*. 2000: OUP Oxford

7. Howl, J., *Peptide Synthesis and Applications*. 2005: Humana Press

8. Hancock, W. S.; Prescott, D. J.; Vagelos, P. R.; Marshall, G. R., J. Org. Chem., 1973, 38, 774-781; Westall, F. C.; Robinson, A. B., J. Org. Chem., 1970, 35, 2842-2844; Kent, S. B. H.; Merrifield, R. B., Peptides 1980 (K. Brunfeldt Ed), Pierce Chemical Company, Rockford, IL, pp 328-333.

9. Markvoort A. J. , Theoretical models of nonlinear effects in two-component cooperative supra molecular copolymerizations.

10. Sontz,., W.J. Song, and F.A. Tezcan, *Interfacial metal coordination in engineered protein and peptide assemblies.* Current Opinion in Chemical Biology, 2014. **19**(0): p. 42-49.

11. Zastrow, M.L., et al., *Hydrolytic catalysis and structural stabilization in a designed metalloprotein.* Nat Chem, 2012. **4**(2): p. 118-123

12. Niece, K.L., et al., *Self-Assembly Combining Two Bioactive Peptide-Amphiphile Molecules into Nanofibers by Electrostatic Attraction.* Journal of the American Chemical Society, 2003. **125**(24): p. 7146-7147.

13. Yasa, I. Ceren, et al. "Basal Lamina Mimetic Nanofibrous Peptide Networks for Skeletal Myogenesis." *Scientific reports* 5 (2015).

14. Koolman, J. and K.H. Roehm, *Color Atlas of Biochemistry*. 2011: Thieme.

15. P. Xue, R. Lu, G. Chen, Y. Zhang, H. Nomoto, M. Takafuji, H. Ihara, *Chem. Eur. J.* 2007, *13*, 8231.

16. JT. Tu, X. L. Bao, W. Assenmacher, H. Peterlik, J. Daniels, K. H. Dotz, *Chem. Eur. J.* 2009, *15*, 1853.

17. M. Suzuki, M. Yumoto, H. Shirai, K. Hanabusa, *Chem. Eur. J.* 2008, *14*, 2133.

18. J. K. H. Hui, Z. Yu, M. J. MacLachlan, *Angew. Chem. Int. Ed. Engl.* 2007, *46*, 7980.

19. S. T. Lam, G. Wang V. W. W. Yam, *Organomet. Chem.* 2008, *27*, 4545.

20. Sargeant, T. D.; Rao, M. S.; Koh, C. Y.; Stupp, S. I. Biomaterials 2008, 29, 1085–1098.

21. A. Gopal, M. Hifsudheen, S. Furumi, M. Takeuchi, A. Ajayaghosh, *Angew. Chem. Int. Ed.* 2012, *51*, 10505.

22. S. R. Nam, H. Y. Lee, J. I. Hong, *Chem. Eur. J.* 2008, *14*, 6040.

23. N. Shi, G. Yin, H. Li, M. Han, Z. Xu, *New J. Chem.* 2008, *32*, 2011.

24. C. L. Zhan, P. Gao, M. H. Liu, *Chem. Commun.* 2005, 462.

25. X. Zhu, Y. Li, P. Duan, M. Liu, *Chem. Eur. J.* 2010, *16*, 8034.

26. Q. Jin, L. Zhang, M. Liu, *Chem. Eur. J.* 2013, *19*, 9234.

27. M. Yamanaka, H. Fujii, *J. Org. Chem.* 2009, *74*, 5390.

28. J. Liu, P. He, J. Yan, X. Fang, J. Peng, K. Liu, Y. Fang, *Adv. Mater.* 2008, *20*, 2508.

29. J. Peng, K. Liu, J. Liu, Q. Zhang, X. Feng, Y. Fang, *Langmuir* 2008, *24*, 2992.

30. Q. Jin, L. Zhang, X. Zhu, P. Duan, M. Liu, *Chem. Eur. J.* 2012, *18*, 4916.

31. S. R. N. H. Y. Lee, J. Hong, *J. Am. Chem. Soc.* 2007, *129*, 1040.

32. M. Dolores Segarra-Maset, V. J. Nebot, J. F. Miravet, B. Escuder, Chem. Soc. Rev. 2013, 42, 7086.

33. H. Cao, P. Duan, X. Zhu, J. Jiang, M. Liu, *Chem. Eur. J.* 2012, *18*, 5546.

34. Hartgerink, J. D.; Beniash, E.; Stupp, S. I. Proc Natl Acad Sci USA 2002, 99, 5133–5138.

35. 35. Guler, M. O.; Claussen, R. C.; Stupp, S. I. J Mater Chem 2005, 15, 4507-4512.

36. Tovar, J. D.; Rabatic, B. M.; Stupp, S. I. Small 2007, 3, 2024–2028

37. Arnold, M. S.; Guler, M. O.; Hersam, M. C.; Stupp, S. I. Langmuir 2005, 21, 4705–4709.

38. Beniash, E.; Hartgerink, J. D.; Storrie, H.; Stendahl, J. C.; Stupp, S. I. Acta Biomater 2005, 1, 387–397

39. Tysseling-Mattiace, V. M.; Sahni, V.; Niece, K. L.; Birch, D.; Czeisler, C.; Fehlings, M. G.; Stupp, S. I.; Kessler, J. A. J Neurosci 2008, 28, 3814–3823.

40. Webber, M. J.; Tongers, J.; Renault, M. A.; Roncalli, J. G.; Losordo, D. W.; Stupp, S. I. Acta Biomater 2009, doi: 10.1016/ j.actbio.2009.07.031.

41. Rajangam, K.; Arnold, M. S.; Rocco, M. A.; Stupp, S. I. Biomaterials 2008, 29, 3298–3305.

42. Rajangam, K.; Behanna, H. A.; Hui, M. J.; Han, X. Q.; Hulvat, J. F.; Lomasney, J. W.; Stupp, S. I. Nano Lett 2006, 6, 2086–2090.

43. Ceylan, H., A. B. Tekinay, and M. O. Guler. "Mussel‐inspired Adhesive Interfaces for Biomedical Applications." Biological and Biomimetic Adhesives: Challenges and Opportunities (2013): 103-116

44. Safont-Sempere, M. M.; Osswald, P.; Stolte, M.; Grune, M.; Renz, M.; Kaupp, M.; Radacki, K.; Braunschweig, H.; Würthner, F. Impact of Molecular Flexibility on Binding Strength and Self-Sorting of Chiral π-Surfaces. J. Am. Chem. Soc. 2011, 133, 9580−9591.

45. Nagy, K. J.; Giano, M. C.; Jin, A.; Pochan, D. J.; Schneider, J. P. Enhanced Mechanical Rigidity of Hydrogels Formed from Enantio- meric Peptide Assemblies. J. Am. Chem. Soc. 2011, 133, 14975−14977.

46. Shen, Z.; Wang, T.; Liu, M. Tuning The Gelation Ability of Racemic Mixture by Melamine: Enhanced Mechanical Rigidity and Tunable Nanoscale Chirality. Langmuir 2014, 30, 10772−10778.

47. Brizard, A.; Aime, C.; Labrot, T.; Huc, I.; Berthier, D.; Artzner, F.; Desbat, B.; Oda, R. Counterion, Temperature, and Time Modulation of Nanometric Chiral

Ribbons from Gemini-Tartrate Amphiphiles. J. Am. Chem. Soc. 2007, 129, 3754−3762.

48. Zhu, X.; Li, Y.; Duan, P.; Liu, M. Self-Assembled Ultralong Chiral Nanotubes and Tuning of Their ChiralityThrough the Mixing of Enantiomeric Components. Chem.焐Eur. J. 2010, 16, 8034−8040.

49. Hegstrom, R. A.; Kondepudi, D. K. The Handedness of the Universe. Sci. Am. 1990, 262, 108−115.

50. Shen, Z.; Wang, T.; Liu, M. Macroscopic Chirality of Supramolecular Gels Formed from Achiral Tris(Ethyl Cinnamate) Benzene-1,3,5-Tricarboxamides. Angew. Chem., Int. Ed. 2014, 53, 13424−13428.

51. Palmans, A. R. A.; Vekemans, J.; Hikmet, R. A.; Fischer, H.; Meijer, E. W. Lyotropic Liquid-Crystalline Behavior in Disc-Shaped Compounds Incorporating the 3,3′ -Di(Acylamino)-2,2′ -Bipyridine Unit. Adv. Mater.1998, 10, 873−876.

52. 52. Danila, I.; Riobe, F.; Piron, F.; Puigmarti-Luis, J.; Wallis, J. D.; Linares, M.; Ågren, H.; Beljonne, D.; Amabilino, D. B.; Avarvari, N. C3-Symmetrical Supramolecular Architectures: Fibers and Organic Gels from Discotic Trisamides and Trisureas. J. Am. Chem. Soc. 2011, 133, 8344−8353.

53. Palmans, A. R. A.; Vekemans, J.; Havinga, E. E.; Meijer, E. W. Sergeants-And-Soldiers Principle in Chiral Columnar Stacks of Disc-ShapedMoleculesWithC3Symmetry.Angew.Chem.,Int.Ed.1997,36, 2648−2651.

54. Palmans, A. R.; Meijer, E. W. Amplification of Chirality in Dynamic Supramolecular Aggregates. Angew. Chem., Int. Ed. 2007, 46, 8948−8968.

55. Lifson, S.; Andreola, C.; Peterson, N. C.; Green, M. M. Macromolecular Stereochemistry-Helical Sense Preference in Optically- Active Polyisocyanates-Amplification of a Conformational Equilibrium Deuterium-Isotope Effect. J. Am. Chem. Soc. 1989, 111, 8850−8858.

56. Markvoort A. J. , Theoretical models of nonlinear effects in two-component cooperative supramolecular copolymerizations

57. Liu, Minghua, Li Zhang, and Tianyu Wang. "Supramolecular Chirality in Self-Assembled Systems." *Chemical Reviews* 115.15 (2015): 7304-7397.

58. 58. Cui, Honggang, Matthew J. Webber, and Samuel I. Stupp. "Self‐assembly of peptide amphiphiles: From molecules to nanostructures to biomaterials."Peptide Science 94.1 (2010): 1-18.

59. Marchesan, S.; Easton, C. D.; Styan, K. E.; Waddington, L. J.; Kushkaki, F.; Goodall, L.; McLean, K. M.; Forsythe, J. S.; Hartley, P. G. Chirality Effects at Each Amino Acid Position on Tripeptide Self- Assembly into Hydrogel Biomaterials. Nanoscale 2014, 6, 5172−5180.

60. Liu, G.-F.; Zhang, D.; Feng, C.-L. Control of Three-Dimensional Cell Adhesion by The Chirality of Nanofibers in Hydrogels. Angew. Chem., Int. Ed. 2014, 53, 7789−7793.

61. Das,R.K.;Zouani,O.F.;Labrugeѐre,C.;Oda,R.;Durrieu,M.-C. Influence of Nanohelical Shape and Periodicity on Stem Cell Fate. ACS Nano 2013, 7, 3351−3361.

62. Jiang, J.; Wang, T.; Liu, M. Creating Chirality in The Inner Walls of Silica Nanotubes Through a Hydrogel Template: Chiral Transcription and Chiroptical Switch. Chem. Commun. 2010, 46, 7178− 7180.

63. Chen, J. C. Introduction to Scanning Tunneling Microscopy; Oxford University Press: New York, 1993.

64. Xu, Q.; Wang, D.; Wan, L.; Wang, C.; Bai, C.; Feng, G.; Wang, M. Discriminating Chiral Molecules of (R)-PPA and (S)-PPA in Aqueous Solution by ECSTM. Angew. Chem., Int. Ed. 2002, 41, 3408−3411.

65. Duan, P.; Zhu, X.; Liu, M. Isomeric Effect in the Self-Assembly of Pyridine-Containing L-Glutamic Lipid: Substituent Position Controlled Morphology and Supramolecular Chirality. Chem. Commun. 2011, 47, 5569−5571.

66. Micsonai, A.,Wien, F.,Kernya, L.,Lee, Y.-H.,Goto, Y.,Réfrégiers, M. Kardos, J., Accurate secondary structure prediction and fold recognition for circular dichroism spectroscopy. Proceedings of the National Academy of Sciences 112, E3095-E3103 (2015).

67. Uzunalli, G., et al. "Bioactive self-assembled peptide nanofibers for corneal stroma regeneration." *Acta biomaterialia* 10.3 (2014): 1156-1166..

68. Paramonov, Sergey E., Ho-Wook Jun, and Jeffrey D. Hartgerink. "Self-assembly of peptide-amphiphile nanofibers: the roles of hydrogen bonding and amphiphilic packing." *Journal of the American Chemical Society* 128.22 (2006): 7291-7298.

69. 69. Salemme, F. R. Prog. Biophys. Mol. Biol. 1983, 42, 95–133.

70. Salemme, F. R.; Weatherford, D. W. J. Mol. Biol. 1981, 146, 101– 117.

71. Lin, Brian F., et al. "pH-responsive branched peptide amphiphile hydrogel designed for applications in regenerative medicine with potential as injectable tissue scaffolds." *Journal of Materials Chemistry* 22.37 (2012): 19447-19454.

72. C. D. M. Churchill and S. D. Wetmore, J. Phys. Chem. B, 2009, 113, 16046–16058.

73. Pashuck, E. Thomas, Honggang Cui, and Samuel I. Stupp. "Tuning supramolecular rigidity of peptide fibers through molecular structure." *Journal of the American Chemical Society* 132.17 (2010): 6041-6046.

74. A. Pasc, F. O. Akong, S. Cosgun and C. Gerardin, Beilstein J. Org. Chem., 2010, 6, 973–977.

75. Zhang, Li, et al. "Tuning Soft Nanostructures in Self‐assembled Supramolecular Gels: From Morphology Control to Morphology‐Dependent Functions." *Small*11.9-10 (2015): 1025-1038